

RESEARCH ARTICLE

# Ddc2<sup>ATRIP</sup> promotes Mec1<sup>ATR</sup> activation at RPA-ssDNA tracts

Himadri Biswas<sup>1</sup>, Greicy Goto<sup>1</sup>, Weibin Wang<sup>2</sup>, Patrick Sung<sup>2,3</sup>, Katsunori Sugimoto<sup>1\*</sup>

**1** Department of Microbiology, Biochemistry and Molecular Genetics, International Center for Public Health, New Jersey Medical School, Rutgers, The State University of New Jersey, Newark, New Jersey, United States of America, **2** Department of Molecular Biophysics and Biochemistry, Yale University School of Medicine, New Haven, Connecticut, United States of America, **3** Department of Biochemistry and Structural Biology, University of Texas Health Science Center at San Antonio, San Antonio, Texas, United States of America

\* [nori.sugimoto@rutgers.edu](mailto:nori.sugimoto@rutgers.edu)



 OPEN ACCESS

**Citation:** Biswas H, Goto G, Wang W, Sung P, Sugimoto K (2019) Ddc2<sup>ATRIP</sup> promotes Mec1<sup>ATR</sup> activation at RPA-ssDNA tracts. *PLoS Genet* 15(8): e1008294. <https://doi.org/10.1371/journal.pgen.1008294>

**Editor:** Lorraine S. Symington, Columbia University, UNITED STATES

**Received:** January 3, 2019

**Accepted:** July 7, 2019

**Published:** August 1, 2019

**Copyright:** © 2019 Biswas et al. This is an open access article distributed under the terms of the [Creative Commons Attribution License](https://creativecommons.org/licenses/by/4.0/), which permits unrestricted use, distribution, and reproduction in any medium, provided the original author and source are credited.

**Data Availability Statement:** All relevant data are within the manuscript and its Supporting Information files.

**Funding:** This work was supported by grant ES007061 (PS) and GM120730 (KS) from National Institute of Health (<http://www.nih.gov>). The funders had no role in study design, data collection and analysis, decision to publish, or preparation of the manuscript.

**Competing interests:** The authors have declared that no competing interests exist.

## Abstract

The DNA damage checkpoint response is controlled by the phosphatidylinositol 3-kinase-related kinases (PIKK), including ataxia telangiectasia-mutated (ATM) and ATM and Rad3-related (ATR). ATR forms a complex with its partner ATRIP. In budding yeast, ATR and ATRIP correspond to Mec1 and Ddc2, respectively. ATRIP/Ddc2 interacts with replication protein A-bound single-stranded DNA (RPA-ssDNA) and recruits ATR/Mec1 to sites of DNA damage. Mec1 is stimulated by the canonical activators including Ddc1, Dpb11 and Dna2. We have characterized the *ddc2-S4* mutation and shown that Ddc2 not only recruits Mec1 to sites of DNA damage but also stimulates Mec1 kinase activity. However, the underlying mechanism of Ddc2-dependent Mec1 activation remains to be elucidated. Here we show that Ddc2 promotes Mec1 activation independently of Ddc1/Dpb11/Dna2 function *in vivo* and through ssDNA recognition *in vitro*. The *ddc2-S4* mutation diminishes damage-induced phosphorylation of the checkpoint mediators, Rad9 and Mrc1. Rad9 controls checkpoint throughout the cell-cycle whereas Mrc1 is specifically required for the S-phase checkpoint. Notably, S-phase checkpoint signaling is more defective in *ddc2-S4* mutants than in cells where the Mec1 activators (Ddc1/Dpb11 and Dna2) are dysfunctional. To understand a role of Ddc2 in Mec1 activation, we reconstituted an *in vitro* assay using purified Mec1-Ddc2 complex, RPA and ssDNA. Whereas ssDNA stimulates kinase activity of the Mec1-Ddc2 complex, RPA does not. However, RPA can promote ssDNA-dependent Mec1 activation. Neither ssDNA nor RPA-ssDNA efficiently stimulates the Mec1-Ddc2 complex containing Ddc2-S4 mutant. Together, our data support a model in which Ddc2 promotes Mec1 activation at RPA-ssDNA tracts.

## Author summary

The ATR-ATRIP complex is recruited to sites of DNA damage by replication protein A-bound single-stranded DNA (RPA-ssDNA), and controls cellular responses to various types of DNA damage. The recruitment of ATR-ATRIP to RPA-ssDNA is not sufficient

for the kinase activation. The activation of ATR-ATRIP requires activators including TopBP1 and ETAA1. In budding yeast, Mec1-Ddc2 (the ATR-ATRIP homolog) is activated through a similar mechanism. Activation of Mec1-Ddc2 requires Ddc1 (Rad9 homolog), Dpb11 (TopBP1 homolog) and Dna2. Our studies of the *ddc2-S4* mutation have shown that Ddc2 promotes not only Mec1 recruitment but also Mec1 activation. In this study we show that Ddc2 promotes Mec1 activation independently of Ddc1/Dpb11/Dna2 function *in vivo*. We also show that Ddc2 regulates Mec1 activation through ssDNA recognition *in vitro*. Although RPA does not directly stimulate Mec1 activity, it can enhance ssDNA-dependent Mec1 activation. Our results suggest that ATR/Mec1, like ATM/Tel1 and DNA-PKcs, is activated upon DNA damage recognition.

## Introduction

Chromosomes are constantly damaged by exogenous and endogenous threats [1]. The repair of damaged chromosomes is therefore critical for maintaining genome stability. The DNA damage response consists of multiple pathways controlled by the phosphatidylinositol 3-kinase-related kinases (PIKK) [2, 3]. These kinases include DNA-dependent protein kinase catalytic subunit (DNA-PKcs), ataxia telangiectasia-mutated (ATM), and ATM and Rad3-related (ATR). Although all these PIKKs respond to DNA damage, their DNA damage specificities are different. ATM and DNA-PKcs are activated by double-stranded DNA breaks (DSBs), whereas ATR responds to various types of DNA lesions with single-stranded DNA (ssDNA) [4, 5].

The Mre11-Rad50-Nbs1 complex recruits and activates ATM at DNA ends [6] whereas the Ku complex recruits and activates DNA-PKcs at DNA ends [3, 7]. The recruitment of ATM and DNA-PKcs is thus coupled to the kinase activation. Replication protein A (RPA) is the major protein that binds ssDNA with a high affinity [8]. ATR interacts with a partner ATRIP and recognizes RPA-covered ssDNA (RPA-ssDNA) [4, 5]. However, the recruitment of the ATR-ATRIP complex (ATR-ATRIP) to RPA-ssDNA is not sufficient for ATR activation. Indeed, ATR-ATRIP is stimulated by checkpoint regulators including TopBP1 and ETAA1 [4, 5]. TopBP1 is recruited to sites of DNA damage or stalled replication forks although the mechanism for the recruitment is not fully understood [9–12]. TopBP1 appears to engage with the Rad9-Rad1-Hus1 (9-1-1) complex at dsDNA-ssDNA junctions [4, 5]. Subsequently, TopBP1 directly stimulates the ATR-ATRIP kinase [4, 5, 13]. ETAA1 interacts with RPA and acts at stalled replication forks [14–16]. Like TopBP1, ETAA1 directly activates ATR-ATRIP [14, 15]. Thus, ATR-ATRIP is recruited by recognizing RPA-ssDNA and subsequently activated through multiple steps [4, 5].

In budding yeast, the Mec1-Ddc2 complex (Mec1-Ddc2) corresponds to ATR-ATRIP [17, 18]. Mec1-Ddc2 interacts with RPA-ssDNA to accumulate at sites of DNA damage [17]. The Ddc1-Mec3-Rad17 complex (the yeast 9-1-1 complex) recruits Dpb11 (TopBP1 ortholog) to the dsDNA-ssDNA junction [19, 20]. In budding yeast, both Ddc1<sup>Rad9</sup> and Dpb11<sup>TopBP1</sup> stimulate Mec1-Ddc2 kinase activity [21–25]. These observations have established the model in which the Ddc1-Dpb11 axis governs the checkpoint pathway by directly activating Mec1-Ddc2. In parallel with the Ddc1-Dpb11 axis, the Dna2 nuclease/helicase stimulates Mec1 kinase activity and controls DNA damage and replication checkpoints in S phase [26]. All Ddc1, Dpb11 and Dna2 proteins utilize the unstructured domains with aromatic amino acid residues (Trp or Tyr) to increase the catalytic activity of Mec1 [23, 24, 26, 27]. Thus, Ddc1, Dpb11 and Dna2 appear to activate Mec1 through a similar mechanism.

In budding yeast, Mec1 activates the downstream kinase Rad53 (Chk2 homolog) to enforce DNA damage checkpoint response [28, 29]. Signal transduction from Mec1 to Rad53 requires checkpoint mediators, such as Rad9 and Mrc1; Mec1 phosphorylates Rad9 and Mrc1 to promote their interaction with Rad53 at sites of DNA damage [30–33]. Rad9 controls checkpoint throughout the cell-cycle whereas Mrc1 is specifically required for the S phase DNA damage checkpoint [28, 32, 34–36]. Mrc1 associates with components of the replication fork in S phase [37, 38]. In contrast, recruitment of Rad9 to sites of DNA damage is a highly regulated process that involves three distinct mechanisms [39, 40]. First, the TUDOR domain of Rad9 interacts with K79-methylated histone H3 [41, 42]. Second, the tandem BRCT domain of Rad9 interacts with S129-phosphorylated histone H2A [43]. Finally, Rad9 binds to the Dpb11 scaffold protein [39, 44]. Histone H3 methylation is a constitutive mark on chromatin [45] and phosphorylated histone H2A spreads over around DNA lesions [46, 47]. However, the Dpb11 scaffold protein localizes to DNA lesions; indeed, Mec1 phosphorylates Ddc1 to promote Ddc1-Dpb11 interaction [39, 44, 48]. Thus, the Ddc1-Dpb11 axis not only stimulates Mec1 kinase activity but also promotes Rad9 recruitment to sites of DNA damage.

We have identified a separation-of-function *ddc2* mutation (*ddc2-S4*) that causes defects in Mec1 activation but does not affect Mec1 recruitment [49]. However, it is not known how Ddc2-dependent Mec1 activation triggers checkpoint signaling. Moreover, the underlying mechanism of Ddc2-dependent Mec1 activation remains to be determined. To understand the significance of Ddc2-dependent Mec1 activation, we further characterized the *ddc2-S4* mutation by carrying out genetic experiments. We found that the *ddc2-S4* mutation impaired Rad9 and Mrc1 phosphorylation after DNA damage, consistent with the previous observation that the *ddc2-S4* mutation is defective in checkpoint activation throughout the cell cycle [49]. The Ddc1-Dpb11 axis and Dna2 contribute to Mec1 activation in S phase [26]. We also found that S-phase checkpoint signaling is more significantly defective in *ddc2-S4* mutants than in *ddc1*- and *dna2*-deficient mutants. Thus, Ddc2 appears to promote Mec1 activation independently of Ddc1/Dpb11 and Dna2 function. We further examined the effect of *ddc2-S4* mutation on kinase activity of Mec1-Ddc2 using an *in vitro* reconstitution system. Whereas ssDNA stimulated Mec1 activity, RPA did not. However, RPA was found to promote ssDNA-dependent Mec1 activation. The Mec1-Ddc2 complex containing Ddc2-S4 mutant (Mec1-Ddc2-S4) exhibited a basal kinase activity *in vitro*. However, neither ssDNA nor RPA-ssDNA efficiently stimulated Mec1-Ddc2-S4. Our results support a model in which Ddc2 promotes Mec1 activation through ssDNA recognition.

## Results

### The *ddc2-S4* mutation impairs Rad9 phosphorylation and recruitment after DNA damage

Mec1 phosphorylates the Rad9 checkpoint mediator to promotes Rad9-Rad53 interaction, which is essential for Rad53 activation [30, 31]. The *ddc2-S4* mutation confers defects in DNA damage checkpoint activation and damage-induced Rad53 phosphorylation at G2/M [49]. To understand the significance of Ddc2-dependent Mec1 activation, we first examined the effect of *ddc2-S4* mutation on Rad9 phosphorylation after DNA damage at G2/M (Fig 1A). Cells expressing HA-tagged Rad9 protein (Rad9-HA) were arrested with nocodazole and exposed to methyl methanesulfonate (MMS). Cells were then subjected to immunoblotting analysis with anti-HA antibodies to monitor Rad9 phosphorylation (Fig 1A). Rad9 underwent phosphorylation in wild-type cells after MMS treatment. Phosphorylation was decreased in *ddc2-S4* mutants but less significantly compared with in *ddc2Δ* mutants. Thus, the *ddc2-S4* mutation impairs Rad9 phosphorylation after DNA damage.

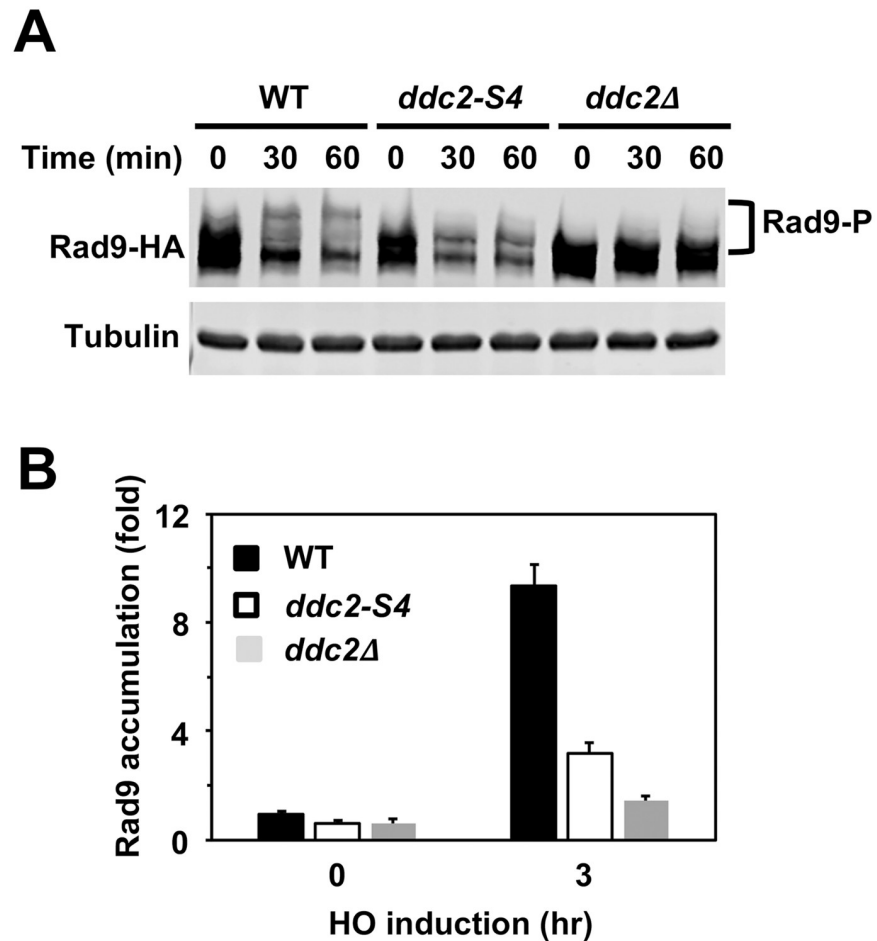


**Fig 1. Effect of *ddc2-S4* or *ddc2Δ* mutation on Rad9 phosphorylation after DNA damage.** (A) Wild-type (HB09), *ddc2-S4* (HB10) or *ddc2Δ* (KSC1536) cells expressing Rad9-HA were treated with nocodazole to arrest at G2/M. Cells were then exposed to 0.05% MMS. Cells were collected at the indicated time points, and extracts were subjected to immunoblotting analysis with anti-HA antibodies or anti-tubulin antibodies. (B) Effect of *ddc2-S4* or *ddc2Δ* on Rad9 localization to a HO-induced DSB. Wild-type (HB09), *ddc2-S4* (HB10) or *ddc2Δ* (KSC1536) cells expressing Rad9-HA were transformed with the YCpA-GAL-HO plasmid. Transformed cells were grown in sucrose and treated with nocodazole. After arrest at G2/M, the culture was incubated with galactose for 3 hr to induce HO expression, while half of the culture was maintained in sucrose to repress HO expression. Cells were subjected to chromatin immunoprecipitation with anti-HA antibodies. Association of Rad9 with a HO-induced DSB was analyzed by real-time PCR. Relative enrichment was determined from three independent experiments. The error bars indicate standard deviation.

<https://doi.org/10.1371/journal.pgen.1008294.g001>

One explanation for Rad9 phosphorylation defect in *ddc2-S4* mutants is that Rad9 does not efficiently localize to sites of DNA damage. We next examined the effect of *ddc2-S4* mutation on Rad9 accumulation at sites of DNA damage by chromatin immunoprecipitation (ChIP) assay (Fig 1B). In budding yeast, HO endonuclease introduces a sequence-specific DSB. We used an experimental system in which cells carry the GAL-HO plasmid and contain a single HO cleavage site at the *ADH4* locus [49]. In this system, HO endonuclease, expressed after incubation with galactose, generates a single DSB at the *ADH4* locus. Cells expressing HA-tagged Rad9 (Rad9-HA) protein were transformed with the GAL-HO plasmid. Transformants were grown initially in sucrose to repress HO expression, and then transferred to medium containing nocodazole to arrest at G2/M. After arrest, galactose was added to induce HO expression. Cells were then analyzed by the ChIP assay using anti-HA antibodies. Rad9

accumulated at sites of DNA damage less efficiently in *ddc2-S4* mutants than in wild-type cells. However, the *ddc2-S4* mutation conferred a milder defect in Rad9 accumulation compared with the *ddc2Δ* mutation (Fig 1B).

Rad9 limits the Sae2- and Sgs1-dependent pathway and interferes with DNA end resection [50]. We next addressed whether the *ddc2-S4* mutation affects the kinetics of DNA end resection. To this end we monitored ssDNA generation at two EcoRI restriction sites near the HO cleavage site (at 0.8 kb or 5.8 kb from the site) by a quantitative PCR-based method [51] (Fig 2A). PCR amplifies only resected DNA because the EcoRI restriction enzyme can cleave unprocessed DNA (S1 Fig). The PCR amplification, normalized to the efficiency of HO cleavage, corresponds to the rate of DNA end resection [51]. The *ddc2-S4* mutation did not significantly affect DNA end resection (Fig 2B). RPA, consisting of Rfa1, Rfa2 and Rfa3, binds to ssDNA tracts [8]. We also examined whether the *ddc2-S4* mutation affects RPA accumulation near the DSB (Fig 2C). No apparent defect in Rfa2 association was observed in *ddc2-S4* mutants. These results support the previous finding that the *ddc2-S4* mutation does not affect Mec1 localization to sites of DNA damage [49]. Our results are also consistent with the current view that Mec1 positively controls DNA end resection although it promotes Rad9 accumulation at sites of DNA damage [52].

Mec1 phosphorylates Ddc1 to recruit Rad9 near sites of DNA damage through the Dpb11 scaffold [39, 44, 48]. We next examined the effect of *ddc2-S4* mutation on Ddc1 phosphorylation after DNA damage (Fig 3A). Cells expressing HA-tagged Ddc1 protein were treated as above and subjected to immunoblotting analysis to monitor Ddc1 phosphorylation. Ddc1 phosphorylation was decreased in *ddc2-S4* mutants compared with wild-type cells. Mec1 and Ddc1 are independently recruited to sites of DNA damage [53, 54]. We confirmed that the *ddc2-S4* mutation has no impact on Ddc1 accumulation at sites of DNA damage (Fig 3B). Thus, the *ddc2-S4* mutation impairs Ddc1 phosphorylation that promotes Ddc1-Dpb11-Rad9 assembly at sites of DNA damage [39, 44, 48].

### The *ddc2-S4* mutation is defective in S phase checkpoint signaling

Mec1 phosphorylates the Mrc1 checkpoint mediator that is essential for Rad53 activation during S phase [32, 35]. Notably, Mrc1-dependent Rad53 activation does not require Rad9 or Ddc1/Dpb11 function [55]. We further examined the effect of *ddc2-S4* mutation on Mrc1 phosphorylation after DNA damage (Fig 4A). Wild-type, *ddc2-S4* or *ddc2Δ* cells expressing HA-tagged Mrc1 protein were arrested in G1 with  $\alpha$ -factor and released into medium containing MMS. Cells were harvested at the indicated times after release. We confirmed that cells remained within S phase at the time point after release (Fig 4A). Mrc1 phosphorylation was decreased in *ddc2-S4* mutants but less significantly than in *ddc2Δ* mutants. Thus, Ddc2-dependent Mec1 activation also controls the Mrc1-dependent checkpoint pathway during S phase.

The Ddc1-Dpb11 axis and Dna2 control DNA damage checkpoints in S phase [26]. Two substitution mutations at the N-terminus of Dna2 (*dna2-W128A, Y130A*; hereafter called *dna2-AA*) abrogate its checkpoint function [26]. We next compared Rad53 phosphorylation in *ddc2-S4*, *ddc2Δ* and *ddc1Δ dna2-AA* mutants in S phase (Fig 4B). Cells expressing HA-tagged Rad53 protein were arrested at G1 and released into MMS or hydroxyurea (HU) as above. Rad53 phosphorylation was decreased in *ddc1Δ dna2-AA* mutants. However, a more significant defect was observed in *ddc2-S4* or *ddc2Δ* mutants (Fig 4B). Our results agree with the previous observation that *ddc1Δ dna2-AA* cells are less defective in Rad53 activation than *mec1Δ* cells [56]. We next compared DNA damage sensitivity of *ddc2-S4* and *ddc1Δ dna2-AA* mutants. While the *ddc2-S4* and the *ddc1Δ dna2-AA* mutation caused similar sensitivities to MMS, *ddc2-S4* mutants were more sensitive to HU than *ddc1Δ dna2-AA* mutants (Fig 4C).

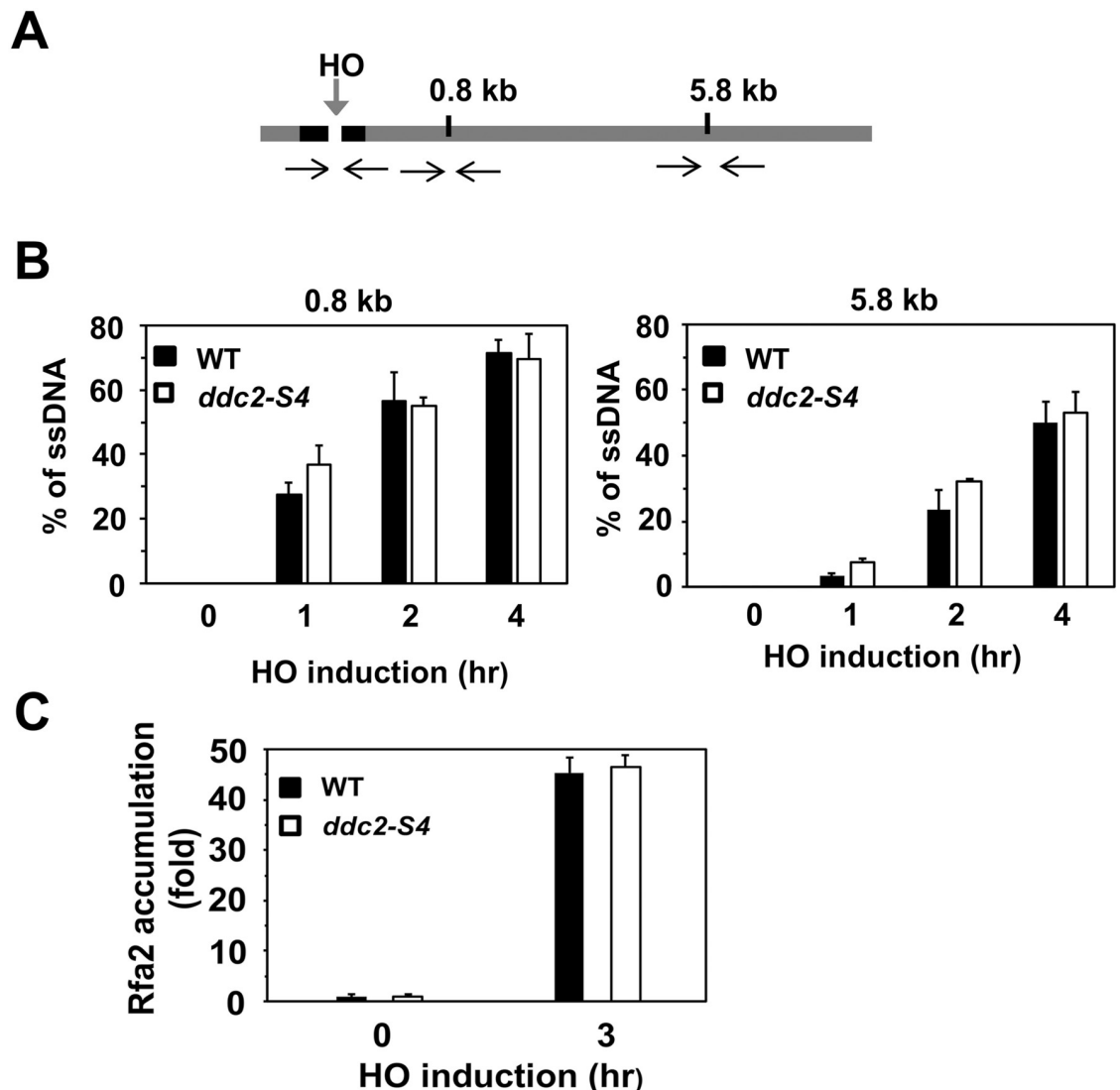


**Fig 2. Effect of *ddc2-S4* mutation on DNA end resection and RPA accumulation.** (A) Scheme of the *ADH4* locus containing a HO cleavage site. One EcoRI restriction site is located 0.8 kb away from the HO cleavage site whereas another is 5.8 kb away. The black arrows indicate PCR primer pairs to monitor HO or EcoRI cleavage. (B) Effect of *ddc2-S4* mutation on DNA end resection. Wild-type (HB01) or *ddc2-S4* (HB02) cells carrying YCPA-GAL-HO were grown in sucrose and treated with nocodazole. After arrest at G2/M, the culture was incubated with galactose to induce HO expression. Cells were collected at the indicated times for genomic DNA preparation. Genomic DNA was digested with EcoRI and analyzed by real-time PCR. Experiments were carried out three times. The error bars indicate standard deviation. (C) Effect of *ddc2-S4* on Rfa2 localization to a HO-induced DSB. Wild-type (HB01) or *ddc2-S4* (HB02) cells were transformed with the YCPA-GAL-HO plasmid. Transformed cells were grown in sucrose and treated with nocodazole. The culture was then incubated with galactose for 3 hr to induce HO expression, while half of the culture was maintained in sucrose to repress HO expression. Cells were subjected to chromatin immunoprecipitation with anti-Rfa2 antibodies. Association of Rfa2 with a HO-induced DSB was analyzed by real-time PCR. Relative enrichment was determined from three independent experiments. The error bars indicate standard deviation.

<https://doi.org/10.1371/journal.pgen.1008294.g002>

We further addressed whether the residual checkpoint activation in *ddc1Δ dna2-AA* mutants depends on Mec1 function in S phase (Fig 4D). The introduction of a *mec1Δ* mutation decreased damage-induced Rad53 phosphorylation in *ddc1Δ dna2-AA* mutants. Together, these results suggest that Ddc2 promotes Mec1 activation through a Ddc1/Dpb11/Dna2-independent mechanism.

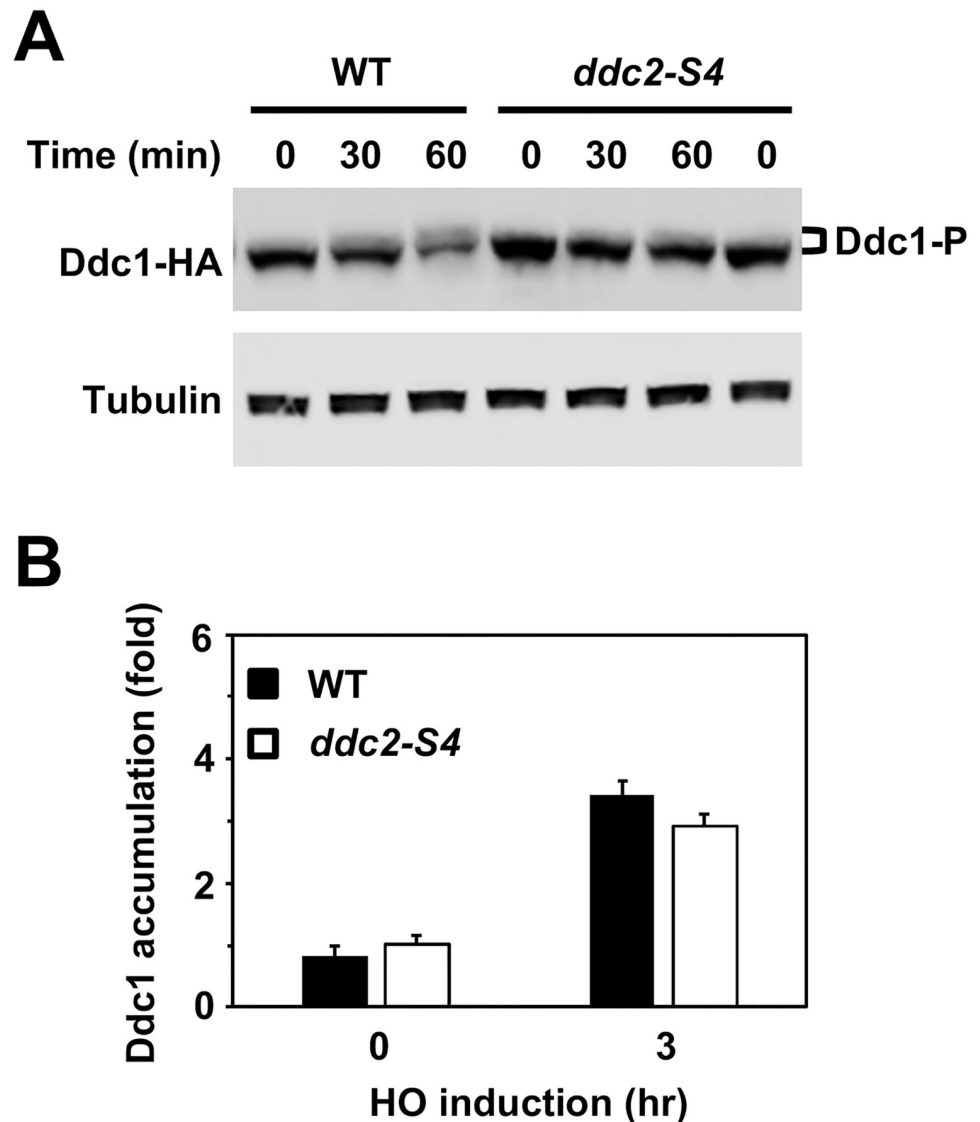


**Fig 3. Effect of *ddc2-S4* on Ddc1 phosphorylation and localization in response to DNA damage.** (A) Effect of *ddc2-S4* mutation on Ddc1 phosphorylation after DNA damage. Wild-type (HB12) or *ddc2-S4* (HB13) cells expressing Ddc1-HA were analyzed as in Fig 1A. (B) Effect of *ddc2-S4* mutation on Ddc1 localization to a HO-induced DSB. Wild-type (HB12) or *ddc2-S4* (HB13) cells expressing Ddc1-HA were transformed with the YCpA-GAL-HO plasmid. Transformed cells were cultured as in Fig 1B and subjected to ChIP assay to monitor Ddc1 localization. Relative enrichment was determined from three independent experiments. The error bars indicate standard deviation from three independent experiments.

<https://doi.org/10.1371/journal.pgen.1008294.g003>

### The *ddc2-S4* mutation is defective in RPA phosphorylation *in vivo* and *in vitro*

Mec1 phosphorylates two subunits of RPA, Rfa1 and Rfa2, in response to DNA damage [57, 58] although the significance of RPA phosphorylation in checkpoint signaling is not fully understood [59]. We examined the effect of *ddc2-S4* mutation on Rfa2 phosphorylation after DNA damage (Fig 5A). Wild-type and *ddc2-S4* mutants were arrested with nocodazole at G2/M and exposed to MMS. Cells were then analyzed by immunoblotting with anti-Rfa2 antibodies. We found that damage-induced Rfa2 phosphorylation was decreased in *ddc2-S4* mutants.

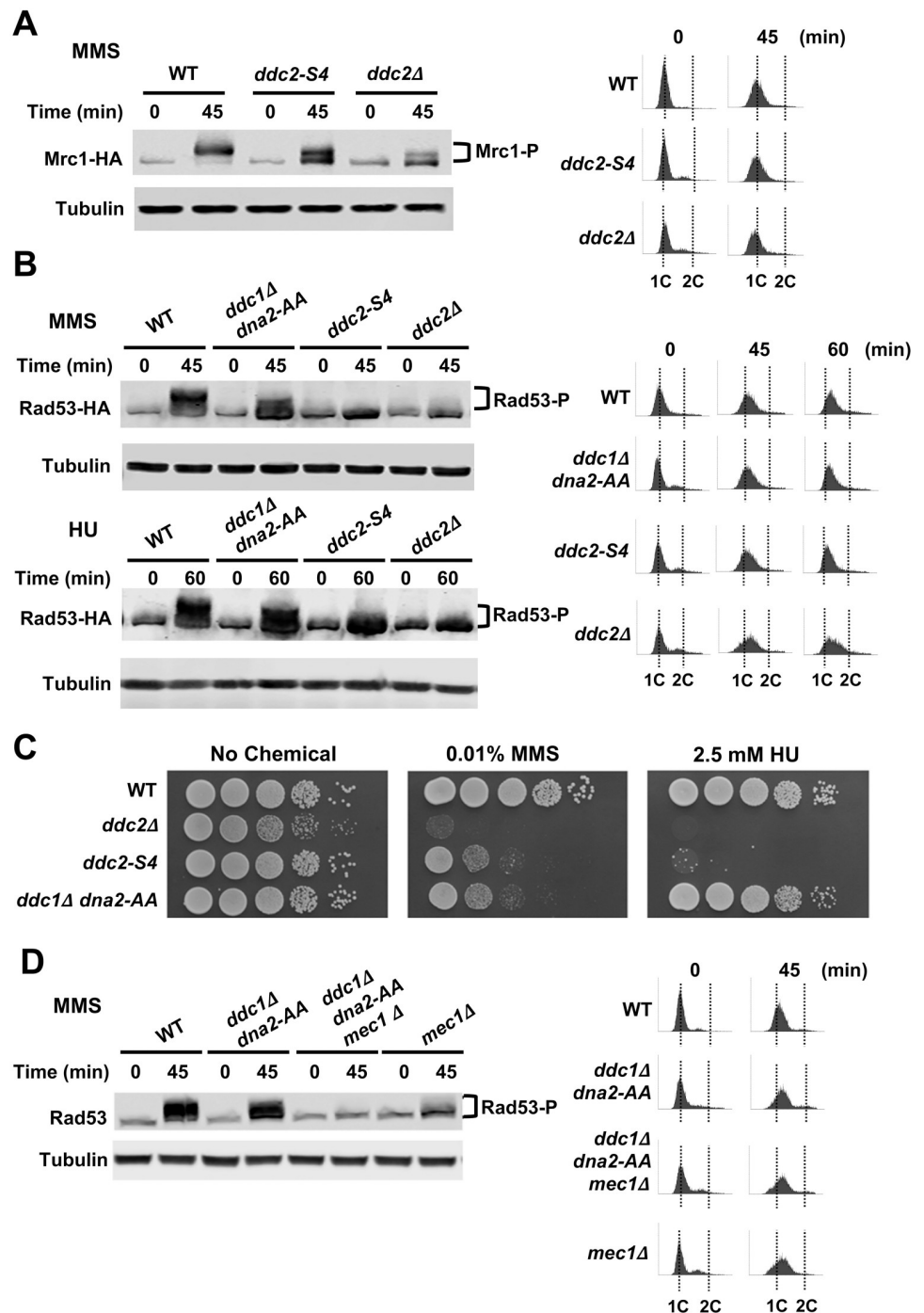


**Fig 4. Effect of *ddc2-S4* mutation on S-phase checkpoint signaling.** (A) Wild-type (KSC4233), *ddc2-S4* (KSC4234) and *ddc2Δ* (KSC4235) cells expressing Mrc1-HA were arrested with  $\alpha$ -factor at G1 and released into medium containing 0.05% MMS. Cells were collected at the indicated time and analyzed as in Fig 1A. Cell cycle progression from G1 to S phase was monitored by DNA flow cytometry. (B) Wild-type (KSC1178), *ddc1Δ dna2-AA* (KSC4219), *ddc2-S4* (KSC3153) and *ddc2Δ* (KSC1234) cells carrying the YCpT-Rad53-HA plasmid were synchronized with  $\alpha$ -factor at G1 and released into medium containing 0.05% MMS or 100 mM HU. Cells were collected at the indicated time (45 min for MMS and 60 min for HU) and analyzed as in Fig 4A. (C) Effect of *ddc1Δ dna2-AA* or *ddc2-S4* on sensitivities to MMS and HU. Wild-type (KSC1178), *ddc1Δ dna2-AA* (KSC4219), *ddc2-S4* (KSC3153) and *ddc2Δ* (KSC1234) cells were serially diluted and spotted on plates medium containing MMS or HU. (D) Wild-type (KSC1178), *ddc1Δ dna2-AA* (KSC4219), *ddc1Δ dna2-AA mec1Δ* (KSC4238) or *mec1Δ* (KSC1186) cells were synchronized with  $\alpha$ -factor at G1 and released into medium containing 0.05% MMS. Cells were collected at the indicated time and subjected to immunoblotting analysis with anti-Rad53 or anti-tubulin antibody. Cell cycle progression from G1 to S phase was monitored by DNA flow cytometry.

<https://doi.org/10.1371/journal.pgen.1008294.g004>



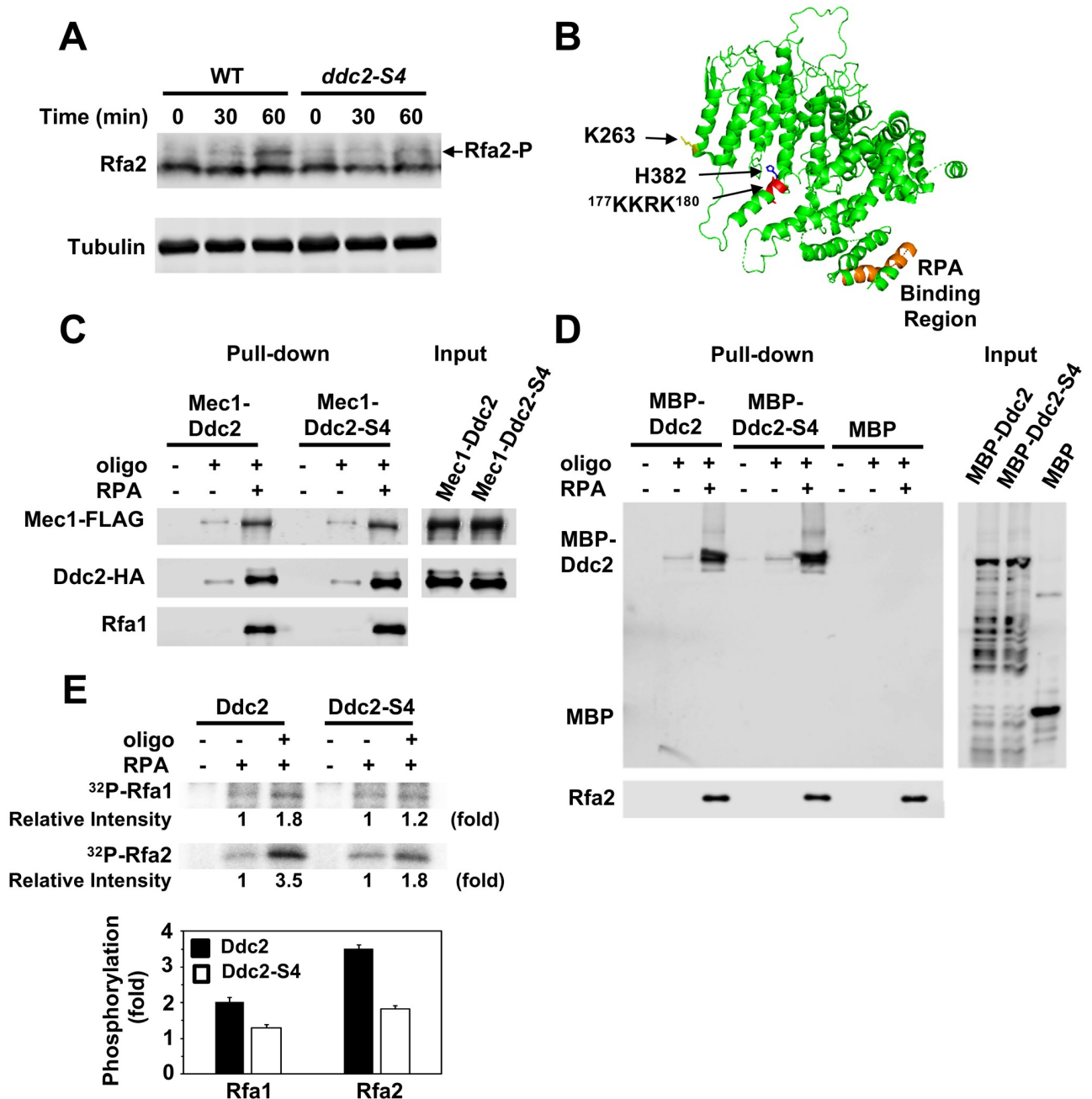


**Fig 5. Effect of *ddc2-S4* mutation on RPA phosphorylation *in vivo* and *in vitro*.** (A) Rfa2 phosphorylation after exposure to MMS. Wild-type (HB01) or *ddc2-S4* (HB02) cells were cultured as in Fig 1A and subjected to immunoblotting analysis with anti-Rfa2 antibodies. (B) Position of the *ddc2-S4* substitution mutation sites. The putative DNA binding (<sup>177</sup>KKRK<sup>180</sup>) and the RPA binding (amino acid 10 to 30) [64] region are highlighted in red and orange, respectively. The side chain of K263 and H382 residues is shown in yellow and blue, respectively. (C) Effect of *ddc2-S4* mutation on ssDNA-binding of Mec1-Ddc2. Streptavidin beads were first incubated with RPA (1 pmol) or bio-oligo(dN)<sub>80</sub> (5 pmol). Beads were further incubated with Mec1-Ddc2 or Mec1-Ddc2-S4 (0.5 pmol). Captured proteins on beads were detected by immunoblotting with anti-FLAG, anti-HA or anti-Rfa1 antibodies. Note that Mec1 is FLAG-tagged and Ddc2 is HA-tagged. (D) Effect of *ddc2-S4* mutation on ssDNA-binding of Ddc2. Streptavidin beads were first incubated with RPA (1 pmol) or bio-oligo(dN)<sub>80</sub> (5 pmol). Beads were further incubated with MBP, MBP-Ddc2 or MBP-Ddc2-S4 (0.5 pmol). MBP or MBP-fusion proteins were prepared from *E. coli*. Captured proteins on beads were analyzed by immunoblotting with anti-MBP or anti-Rfa2 antibodies. (E) Effect of *ddc2-S4* mutation on RPA phosphorylation *in vitro*. Kinase reactions were carried out with Mec1-Ddc2 or Mec1-Ddc2-S4 (5 nM) in the absence or the presence of RPA (10 nM) or bio-oligo(dN)<sub>80</sub> (125 nM). Incorporation of <sup>32</sup>P into Rfa1 and Rfa2 were normalized to that observed with Rfa1 and Rfa2 alone. The error bars indicate standard deviation from three independent experiments.

<https://doi.org/10.1371/journal.pgen.1008294.g005>

The *ddc2-S4* mutation does not affect Mec1 or RPA accumulation at sites of DNA damage [49] (Fig 2C). Thus, the *ddc2-S4* mutation impairs Rfa2 phosphorylation *in vivo*.

Mec1/ATR phosphorylates RPA efficiently in the presence of ssDNA *in vitro* [21, 58, 60]. However, whether RPA or ssDNA modulates ATR/Mec1 activity remains to be determined. To understand a role of Ddc2 in Mec1 activation, we reconstituted an *in vitro* system using purified Mec1-Ddc2 and RPA proteins. We have purified Mec1-Ddc2 and Mec1-Ddc2-S4 through a two-step affinity chromatography after overexpressing FLAG-tagged Mec1 and His-tagged Ddc2 protein in yeast cells (S2 and S3 Figs). In agreement with the previous studies [21, 58], Mec1-Ddc2 phosphorylated RPA efficiently in the presence of ssDNA (S4 Fig).

The *ddc2-S4* mutation contains two substitution mutations (K263E, H382Y). K263 is implicated in Mec1-Ddc2 homodimerization [61] whereas H382 is in close proximity to the <sup>177</sup>KKRK<sup>180</sup> motif which is involved in DNA binding [61, 62] (Fig 5B, S5 Fig). Ddc2/ATRIP itself interacts weakly with ssDNA but RPA stimulates ssDNA binding of Ddc2/ATRIP [17, 62]. We determined the effect of *ddc2-S4* mutation on the interaction of Mec1-Ddc2 with ssDNA or RPA-ssDNA by a pull-down assay. Mec1-Ddc2 and Mec1-Ddc2-S4 were found to bind similarly to ssDNA or RPA-ssDNA *in vitro* (Fig 5C), consistent with the observation that the *ddc2-S4* mutation does not affect Mec1 accumulation at sites of DNA damage [49]. We further examined the effect of *ddc2-S4* mutation on Ddc2-ssDNA binding. We prepared MBP-fused Ddc2 or Ddc2-S4 from *E. coli* and further examined whether they interact with oligonucleotides in the presence or absence of RPA (Fig 5D). MBP-Ddc2 and MBP-Ddc2-S4 interacted similarly with ssDNA and RPA-ssDNA. MBP alone did not exhibit oligonucleotide binding (Fig 5D). Thus, the *ddc2-S4* mutation does not affect its own ssDNA- or RPA-ssDNA-binding abilities.

We next examined whether Mec1-Ddc2-S4, like Mec1-Ddc2, phosphorylates RPA efficiently in the presence of ssDNA (Fig 5E). Mec1-Ddc2 and Mec1-Ddc2-S4 similarly phosphorylated Rfa2 in the absence of ssDNA. However, in the presence of ssDNA, Mec1-Ddc2-S4 phosphorylated Rfa2 less efficiently compared with Mec1-Ddc2 (Fig 5E). A similar defect in Rfa1 phosphorylation was observed with Mec1-Ddc2-S4 (Fig 5E). Together, these results raise a possibility that Ddc2 upregulates Mec1 kinase activity by interacting with ssDNA or RPA-ssDNA.

### ssDNA, but not RPA, stimulates Mec1 activity in a Ddc2-dependent manner

We addressed whether RPA or ssDNA regulates Mec1 activity using GST-Rad53 as a substrate (Fig 6). GST-Rad53 lacks the N-terminal kinase domain of Rad53; therefore, no phosphorylation into GST-Rad53 was observed without Mec1-Ddc2 [49] (Fig 6A and 6B). We first tested the effect of various concentrations of RPA on Mec1 kinase activity. RPA had no significant impact on Mec1 activity using GST-Rad53 as a substrate (Fig 6A).

We next investigated the effect of ssDNA on Mec1 activity using various lengths (20, 40, 60 or 80 mer) of oligo(dT) (Fig 6B and 6C). Although no apparent stimulation was observed with a 20 mer oligo(dT) (oligo(dT)<sub>20</sub>), longer oligonucleotides, oligo(dT)<sub>40</sub>, oligo(dT)<sub>60</sub> and oligo(dT)<sub>80</sub>, were found to increase Mec1 activity more efficiently. Similar activation was observed with oligo(dT)<sub>80</sub> and an 80-mer biotinylated oligonucleotide containing all DNA bases (bio-oligo(dN)<sub>80</sub>) (Fig 6C). We note that biotinylation of oligonucleotide has no impact on Mec1 activation (S6 Fig). High concentrations of 80-mer oligonucleotides (125 nM) were required to reach maximum activation compared with the concentration of Mec1 (5 nM). We further tested whether longer ssDNA stimulates Mec1 more strongly using 5 kb ΦX174 phage ssDNA (Fig 6D). A single-stranded form of ΦX174 phage stimulated Mec1 at much lower

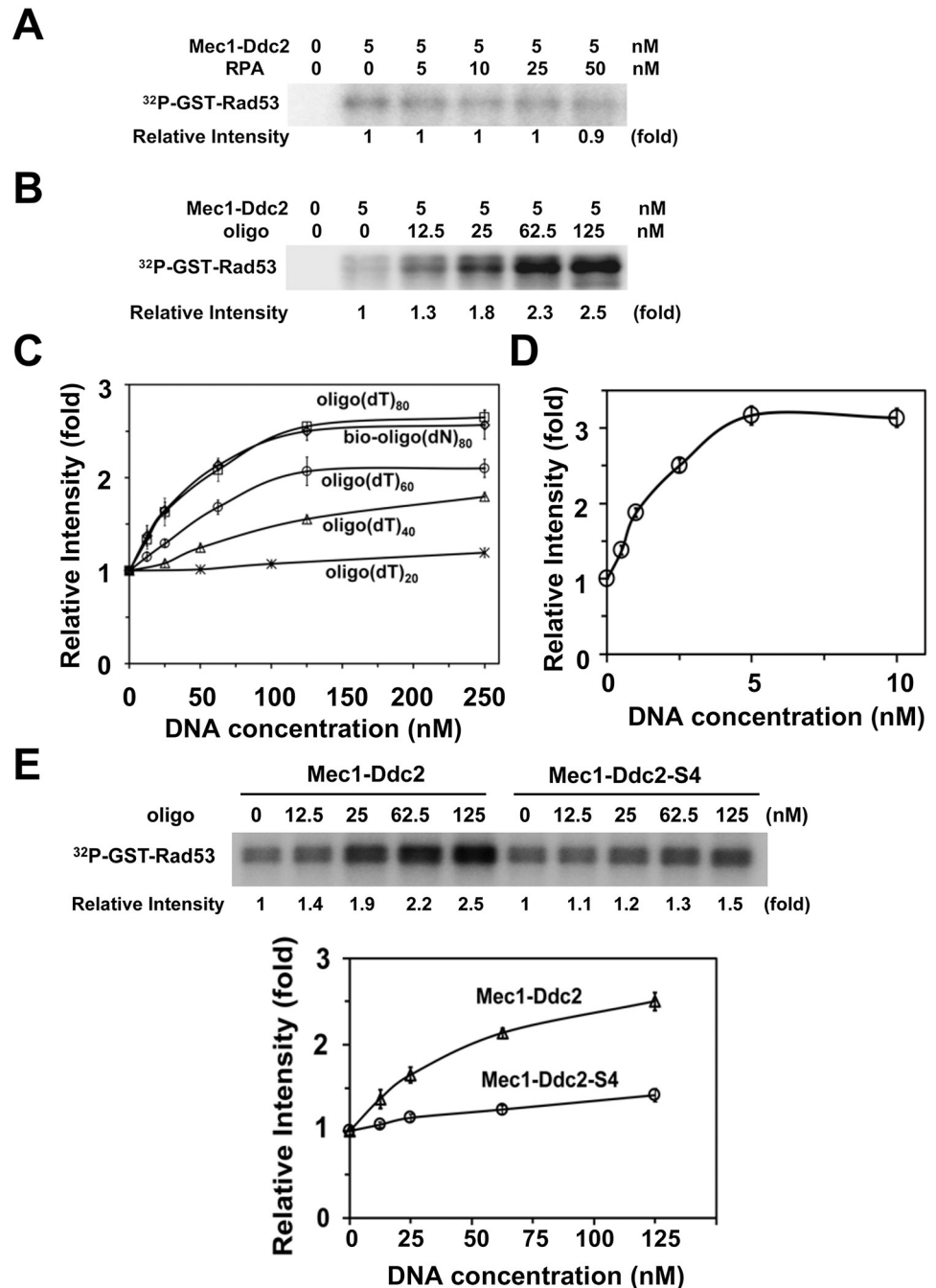


**Fig 6. Effect of RPA or ssDNA addition on Mec1 activity.** (A) Effect of RPA addition on Mec1 catalytic activity. Kinase reactions were carried out with or without Mec1-Ddc2 (5 nM) using various concentrations of RPA. GST-Rad53 C-terminus fusion (GST-Rad53) was used as a substrate of Mec1. Incorporation of <sup>32</sup>P into GST-Rad53 was detected by phosphor imaging. The Rad53 C-terminus does not contain its kinase domain; phosphorylation of GST-Rad53 depends on Mec1-Ddc2. Phosphorylation levels of GST-Rad53 were normalized to that observed with Mec1-Ddc2 alone. The error bars indicate standard deviation from three independent experiments. (B) Effect of ssDNA addition on Mec1 catalytic activity. Kinase reactions were carried out with or without Mec1-Ddc2 (5 nM) using various concentrations of 80-mer biotin-oligo(dN)<sub>80</sub>. Incorporation of <sup>32</sup>P into GST-Rad53 was analyzed as in A. The error bars indicate standard deviation from three independent experiments. (C, D) Effect of length and base-composition of ssDNA on Mec1 activation. Mec1-Ddc2 complex (5 nM) was incubated with various concentrations of oligonucleotides (20, 40, 60, 80-mer oligo(dT), 80-mer bio-oligo(dN)<sub>80</sub> (C) or ΦX phage ssDNA (5 kb) (D). Phosphorylation of GST-Rad53 was normalized to that observed without RPA or ssDNA. The error bars indicate standard deviation from three independent experiments. (E) Effect of *ddc2-S4* mutation on Mec1 activation

by ssDNA. Kinase reactions were carried out with Mec1-Ddc2 or Mec1-Ddc2-S4 (5 nM) using various concentrations of bio-oligo(dN)<sub>80</sub>. Incorporation of <sup>32</sup>P into GST-Rad53 was analyzed as in A. The error bars indicate standard deviation from three independent experiments.

<https://doi.org/10.1371/journal.pgen.1008294.g006>

concentrations compared with 80-mer oligonucleotides. The maximum activation obtained with  $\Phi$ X (3 fold) was slightly higher than that of 80-mer oligonucleotides (2.5 fold) (Fig 6C and 6D). These results indicate that ssDNA stimulates Mec1 in a dosage-dependent and length-dependent manner.

We then determined the effect of *ddc2-S4* mutation on ssDNA-dependent Mec1 activation using 80-mer oligonucleotides (Fig 6E). Mec1-Ddc2-S4 and Mec1-Ddc2 exhibited similar basal kinase activities. However, Mec1-Ddc2-S4 was not efficiently stimulated by ssDNA. Thus, ssDNA appears to stimulate Mec1 activity through a Ddc2-dependent mechanism.

### RPA modulates ssDNA-dependent Mec1 activation *in vitro*

We next determined the combination effect of RPA and ssDNA on Mec1 kinase activity using GST-Rad53 as a substrate. RPA prompts ssDNA binding of Mec1-Ddc2 or Ddc2 (Fig 5C and 5D) whereas ssDNA stimulates Mec1 kinase activity (Fig 6). We thus expected that RPA promotes ssDNA-dependent Mec1 activation. However, Mec1-Ddc2 was found to interact with RPA independently of ssDNA *in vitro*, in agreement with the current view that the N-terminus of Rfa1 interacts directly with the N-terminus of Ddc2 [63, 64] (Fig 7A). Therefore, RPA by itself could compete with ssDNA-bound RPA for Mec1-Ddc2 binding (S7 Fig). Moreover, RPA is a good substrate of Mec1 (S4 Fig); that is, RPA could compete with GST-Rad53 as a Mec1 substrate [65]. Hence, high RPA concentrations could have negative impacts on ssDNA-dependent Mec1 activation *in vitro*.

We first examined the effect of RPA on Mec1 activation with a low concentration of 80-mer oligonucleotides (12.5 nM) (Fig 7B). We note that only weak Mec1 activation was observed at this concentration (Fig 6B and 6C). We incubated oligonucleotides with various concentrations of RPA and subsequently with Mec1-Ddc2 to initiate the kinase reaction. Lower concentrations of RPA enhanced Mec1 kinase activity whereas higher concentrations of RPA attenuated (Fig 7B and 7D). We further tested the effect of RPA on Mec1 activation with a higher concentration of oligonucleotide (125 nM) (Fig 7C). Again, lower concentrations of RPA stimulated Mec1 activity whereas higher concentrations of RPA attenuated. These results are consistent with the hypothesis that RPA promotes ssDNA-dependent Mec1 activation although high RPA concentrations have negative impacts on ssDNA-dependent Mec1 activation *in vitro*. The stimulatory effect of RPA was less pronounced when Mec1-Ddc2 was incubated with a higher concentration of oligonucleotides (Fig 7C and 7D), consistent with the observation that ssDNA, but not RPA, stimulates Mec1-Ddc2 activity (Fig 6).

As discussed above, the *ddc2-S4* mutation causes a defect in ssDNA-dependent Mec1 activation (Fig 6E) although it does not affect RPA-ssDNA binding of Mec1-Ddc2 (Fig 5C and 5D). We then determined the effect of *ddc2-S4* mutation on Mec1 activation in the presence of oligonucleotides (12.5 nM) and RPA (0, 5, 10 nM) (Fig 7E). Mec1-Ddc2-S4, unlike Mec1-Ddc2, was not efficiently stimulated by RPA-ssDNA (Fig 7E). Together, our results support a model in which Ddc2 mediates Mec1 activation through ssDNA recognition while RPA prompts ssDNA binding of Mec1-Ddc2 at sites of DNA damage.

### Discussion

Previous studies have established the model in which ATRIP/Ddc2 interacts with RPA-coated ssDNA and recruits ATR/Mec1 to sites of DNA damage [4, 5]. However, Ddc2 appears to

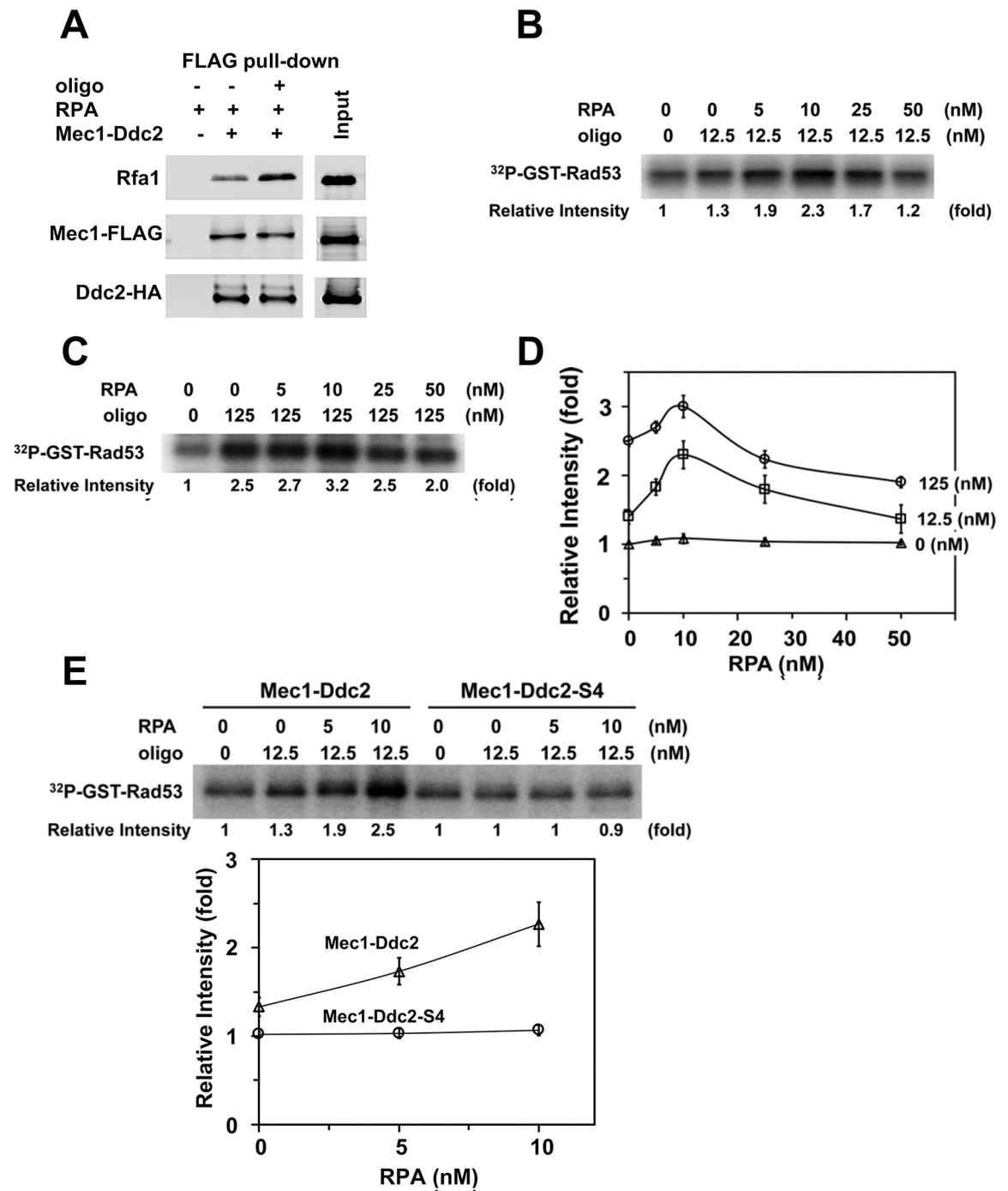


**Fig 7. Effects of RPA on ssDNA-dependent Mec1 activation.** (A) Interaction of Mec1-Ddc2 with RPA in the presence or absence of ssDNA. Mec1-Ddc2 (0.5 pmol) and RPA (1 pmol) were incubated with ANTI-FLAG-M2 agarose in the presence or absence of bio-oligo (dN)<sub>80</sub> (5 pmol). Proteins bound to ANTI-FLAG-M2 agarose were analyzed by immunoblotting analysis with anti-FLAG, anti-HA or anti-Rfa1 antibodies. Note that Mec1 is FLAG-tagged and Ddc2 is HA-tagged. (B) Effect of RPA addition on Mec1 activation in the presence of low concentrations of ssDNA. Kinase reactions were carried out with Mec1-Ddc2 (5 nM) using various concentrations of RPA in the absence or presence of bio-oligo(dN)<sub>80</sub> (12.5 nM). Incorporation of <sup>32</sup>P into GST-Rad53 was analyzed as in Fig 6A. Kinase activities of Mec1-Ddc2, normalized to that observed with Mec1-Ddc2 alone, are shown in comparison with those in the presence of RPA or ssDNA. Experiments were carried out three times and the representative result is shown. (C) Effect of RPA on Mec1 activity in the presence of high concentrations of ssDNA. Kinase reactions were carried out with Mec1-Ddc2 (5 nM) using various concentrations of RPA in the absence or presence of bio-oligo(dN)<sub>80</sub> (125 nM). Incorporation of <sup>32</sup>P into GST-Rad53 was analyzed as in Fig 6A. Kinase activities of Mec1-Ddc2, normalized to that observed with Mec1-Ddc2 alone, are shown in comparison with those in the presence of

RPA or ssDNA. Experiments were carried out three times and the representative result is shown. (D) Effects of RPA concentrations on ssDNA-dependent Mec1 activation. Kinase activities of Mec1-Ddc2 using various concentrations of RPA in the presence of bio-oligo (dN)<sub>80</sub> (12.5 nM or 125 nM) were normalized to that observed with Mec1-Ddc2 alone (See Fig 7B or 7C, respectively). Relative kinase activities with various concentrations of RPA in the absence of ssDNA are also included (see Fig 6A). The error bars indicate standard deviation from three independent experiments. (E) Effect of *ddc2-S4* mutation on Mec1 activation by RPA and ssDNA. Kinase reactions were carried out with Mec1-Ddc2 or Mec1-Ddc2-S4 (5 nM) using various concentrations of RPA in the absence or the presence of bio-oligo(dN)<sub>80</sub> (12.5 nM). Incorporation of <sup>32</sup>P into GST-Rad53 was analyzed as in Fig 6A. The error bars indicate standard deviation from three independent experiments.

<https://doi.org/10.1371/journal.pgen.1008294.g007>

stimulate Mec1 kinase activity at sites of DNA damage [49]. In this study we have further characterized the *ddc2-S4* mutation by carrying out genetic and biochemical experiments. The *ddc2-S4* mutation causes defects in phosphorylation and accumulation of the Rad9 checkpoint mediator at sites of DNA damage. The *ddc2-S4* mutation also confers a defect in phosphorylation of the S-phase specific Mrc1 checkpoint mediator. The Ddc1-Dpb11 axis and Dna2 contribute to Mec1 activation in S phase [26]. Notably, the *ddc2-S4* mutation causes a more significant defect in S phase checkpoint signaling than the *ddc1Δ dna2-AA* mutation. Thus, Ddc2 controls Mec1 activation through a Ddc1/Dpb11/Dna2-independent mechanism. We further examined the effect of *ddc2-S4* mutation on Mec1 kinase activity using an *in vitro* reconstitution system. ssDNA, but not RPA, stimulates Mec1-Ddc2 kinase activity. However, RPA can promote ssDNA-dependent Mec1 activation. Neither ssDNA nor RPA-ssDNA stimulates Mec1-Ddc2-S4 effectively. Our data support a model in which Ddc2 increases Mec1 kinase activity upon ssDNA recognition.

The *ddc2-S4* mutation confers a defect in Rad9 phosphorylation and accumulation at sites of DNA damage. Mec1 phosphorylates Rad9 to allow Rad9-Rad53 interaction and subsequent Rad53 activation [30, 31, 34]. Rad9 accumulates at sites of DNA damage by interacting with K79-methylated histone H3, S129 phosphorylated histone H2A and the scaffold protein Dpb11 [39, 40]. Mec1 phosphorylates Ddc1 to promote Ddc1-Dpb11-Rad9 interaction at sites of DNA damage [39, 44, 48]. In this study we show that the *ddc2-S4* mutation confers a defect in Ddc1 phosphorylation after DNA damage. We have previously shown that histone H2A phosphorylation is decreased in *ddc2-S4* mutants [49]. Thus, two different Rad9 recruitment mechanisms are defective in *ddc2-S4* mutants. Rad9 recruitment defect may compromise Rad9 phosphorylation in *ddc2-S4* mutants because Mec1 accumulates and phosphorylates Rad9 at sites of DNA damage [30, 31, 34]. Mec1 phosphorylates Dpb11 and enhances the stimulating effect of Dpb11 on Mec1 kinase activity *in vitro* [25, 66]. Similar to Dpb11, Ddc1 directly activates Mec1 kinase *in vitro* [21, 23]. It is not known whether phosphorylated Ddc1 stimulates Mec1 kinase activity more effectively than non-phosphorylated one.

The *ddc2-S4* mutation causes a more significant defect in S phase checkpoint activation than the *ddc1Δ dna2-AA* mutation. Notably, the residual checkpoint activation in *ddc1Δ dna2-AA* cells largely depends on Mec1 function. These results suggest that Ddc2 promotes Mec1 activation through a Ddc1/Dpb11/Dna2-independent mechanism. Mec1 phosphorylates the Mrc1 checkpoint mediator and activates Rad53 in S phase [32, 35]. Notably, Mrc1-dependent Rad53 activation does not require Rad9 or Ddc1/Dpb11 function [55]. Recent evidence suggests that the *dna2-AA* mutation affects DNA replication or repair function rather than checkpoint activation [27]. Thus, Ddc2-dependent Mec1 activation appears to play a key role in the stimulation of the Mrc1 checkpoint pathway during S phase.

The *ddc2-S4* mutation causes a defect in ssDNA-dependent Mec1 activation. Then how does ssDNA stimulate Mec1 kinase activity? Mec1-Ddc2 forms a dimer of heterodimers through multiple interfaces including the PIKK regulatory domain (PRD) [67]. Interestingly, the PRD is closely positioned near the catalytic and activation loop at the kinase

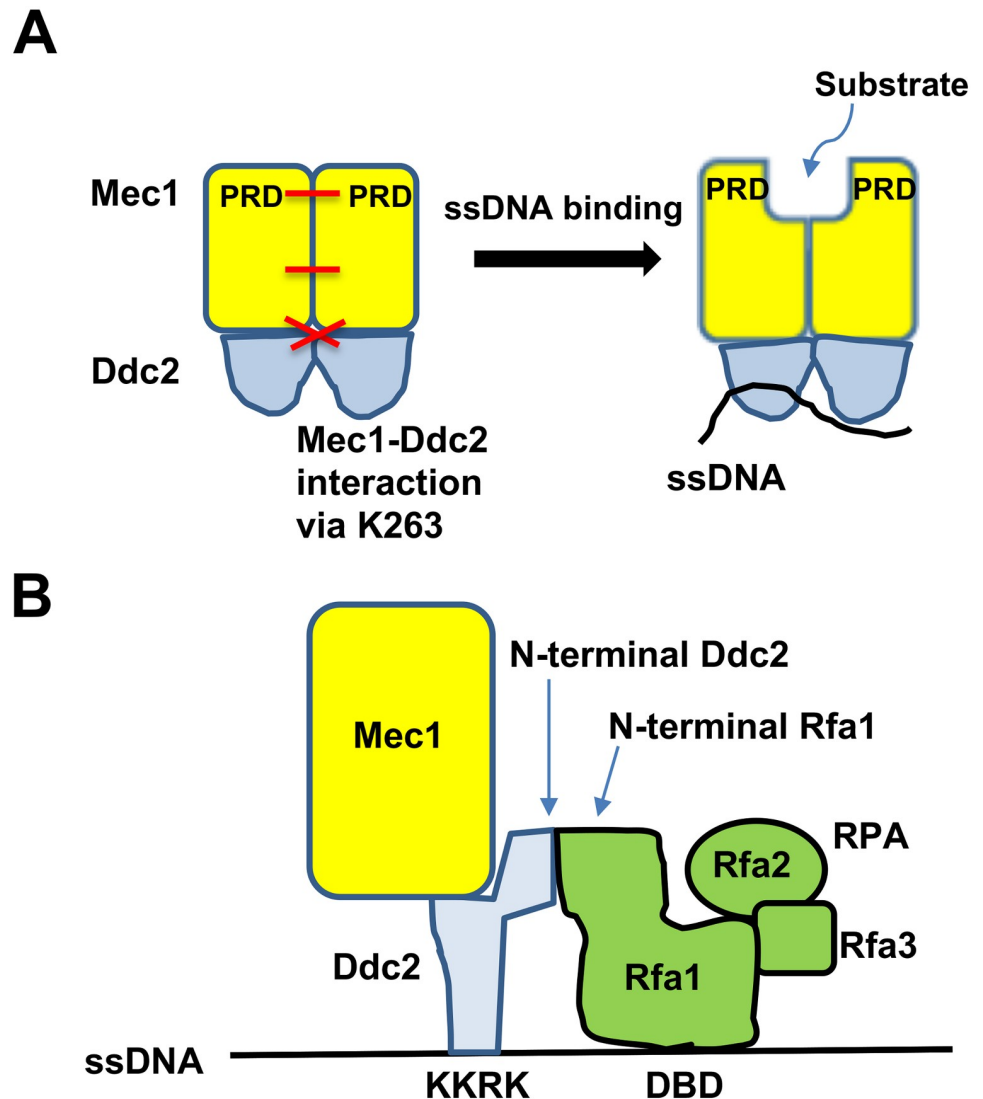


**Fig 8. Model for Mec1 activation at RPA-covered ssDNA tracts.** (A) ssDNA binding of Ddc2 increases Mec1 activity. ssDNA binding of Ddc2 triggers conformation changes of the entire Mec1-Ddc2 homodimer, resulting in structural changes of the kinase domain at the C-terminus of Mec1. K263 is involved in homodimerization of the Mec1-Ddc2 heterodimer. The PRD-PRD interface within the kinase domain is also involved in homodimerization of the Mec1-Ddc2 heterodimer. See text for more detail. (B) RPA promotes ssDNA-dependent Mec1 activation. The N-terminus of Ddc2 interacts with the N-terminus of Rfa1 whereas the DNA binding (KKRK) region of Ddc2 is involved in ssDNA binding. RPA alone binds to ssDNA through its own DNA binding domain (DBD). See the text for more detail.

<https://doi.org/10.1371/journal.pgen.1008294.g008>

domain, thereby blocking kinase activity and substrate entry [61, 67]. We propose that ssDNA binding of Ddc2 triggers conformation changes of the Mec1-Ddc2 homodimer, which could open up the catalytic active site (Fig 8A). The *ddc2-S4* mutation carries two substitution mutations (K263E, H382Y). K263 contributes to Mec1-Ddc2 homodimerization [61] (S5 Fig) whereas H382 is positioned near the putative DNA binding (<sup>177</sup>KKRK<sup>180</sup>) region [61] (Fig 5B). Thus, the *ddc2-S4* mutation may affect conformation changes of Mec1-Ddc2 homodimer upon ssDNA binding. Mec1 phosphorylates Mec1 activators (Ddc1, Dpb11 or Dna2) after DNA damage [66, 68, 69]. Conformation changes of the kinase domain could

therefore enhance binding of Mec1 activators to its own kinase domain. Consistent with the view, Dpb11 has been shown to activate Mec1 more strongly in the presence of RPA and ssDNA [22].

RPA at lower concentrations promotes ssDNA-dependent Mec1 activation *in vitro*. Ddc2 and RPA recognize ssDNA through different mechanisms; the KKRK motif of Ddc2 is implicated in DNA binding [62] whereas RPA utilizes its own DNA binding domain (DBD) [8] (Fig 8B). However, the N-terminus of Ddc2 interacts with RPA independently of ssDNA although other domains of Ddc2 may be involved in RPA interaction [49, 63, 64] (Fig 8B). Thus, RPA-Ddc2 interaction could stimulate Ddc2-ssDNA binding by providing an additional ssDNA-binding interface, thereby boosting ssDNA-dependent Mec1 activation. However, we cannot fully exclude the possibility that RPA, once coated on ssDNA, acquires the ability to directly stimulate Mec1 activity. RPA at higher concentrations attenuates ssDNA-dependent Mec1 activation *in vitro*. One explanation is that RPA by itself competes with RPA-ssDNA for Mec1-Ddc2 binding. Alternatively, there would be substrate competition between RPA and *in vitro* substrates. At the moment, it remains to be determined which property of RPA down-regulates ssDNA-dependent Mec1 activation *in vitro*. Previous *in vitro* studies have shown that RPA-ssDNA has no apparent impact on ATR-ATRIP/Mec1-Ddc2 kinase activity; however, the effect of different RPA concentrations has not been extensively investigated [21, 22, 63, 70]. RPA not only stabilizes ssDNA but also stimulates various repair processes [8, 71–75]. Moreover, RPA binding to ssDNA is highly dynamic using different binding modes [76, 77]. Interestingly, RPA depletion modulates ssDNA generation and Mec1 activation differently [74]. Thus, dynamic interactions between ssDNA, RPA and Mec1-Ddc2 might be important for efficient Mec1 activation. A high-resolution structure of Mec1-Ddc2 has been recently reported [61]. However, the structure and dynamics of how Mec1-Ddc2 and RPA assemble on ssDNA remain to be elucidated.

In summary, we have shown that Ddc2 promotes Mec1 activation independently of Ddc1, Dpb11 and Dna2. We have also provided evidence supporting that Ddc2 promotes Mec1 activation through ssDNA recognition. ATR/Mec1 recognizes RPA-ssDNA and controls many cellular activities during DNA replication and repair [4, 5]. Our studies thus provide insight into how RPA-containing DNA structures modulate ATR/Mec1 activation, and suggest that ATR/Mec1, like DNA-PK and ATM/Tel1, is activated upon the recruitment to sites of DNA damage.

## Experimental procedures

### Strains and plasmids

pRS424-GAL-FLAG-MEC1 is a high-copy plasmid version of YCp/pRS316-GAL-FLAG-MEC1 [78]. The *GAL1-GAL10* promoter region was amplified by PCR with the primer pair 3016 and 3017, fusing a sequence encoding MEHHHHHH to the *GAL1* promoter. The PCR product was cleaved with EcoRI and MluI. The *DDC2* or *ddc2-S4* coding sequence [49] was amplified by PCR with the primer pair KS460 and KSX001, fusing a HA epitope to the N-terminus of Ddc2 or Ddc2-S4, respectively. The PCR product was cleaved with MluI and SalI. The EcoRI-MluI and the MluI-SalI fragments were cloned into YEplac195, generating YEpl95-GAL-His-HA-Ddc2 or YEpl95-GAL-His-HA-Ddc2-S4, respectively. The YCp-T-Rad53-HA plasmid has been described [49]. The *dna2-W128A, Y130A (dna2-AA)* mutation [26] was integrated into the own locus after PCR fusion [79] using primers KS2943, KS2944, KS2955 and KS2946. The *MRC1-HA::TRP1* construct was generated by a PCR-based method [80] using the primer pair KS3649 and KS3650. The strains used in this study are listed in S1 Table.



## DNA end resection assay

Quantitative PCR analysis of DNA end resection was performed as described previously [51]. HO cleaves the HO cut site and generate a DSB. The DNA was digested with the EcoRI restriction enzyme that cleaves the amplicons at 0.8 kb and 5.8 kb from the DSB, but not in the *SMC2* control region. The ssDNA percentage over total DNA was calculated using the following formula: % ssDNA =  $[100/((1+2^{\Delta Ct})/2)]/f$ , in which  $\Delta Ct$  values are the difference in average cycles between digested template and undigested template of a given time point and  $f$  is the HO cut efficiency [51]. HO cutting efficiency was determined as described [81]. The oligonucleotides used are listed in S2 Table.

## Protein purification of Mec1-Ddc2 and Mec1-Ddc2-S4

The yeast strain (*mec1Δ ddc2Δ sml1Δ*; KSC3218) was transformed with pRS424-GAL-FLAG-MEC1 and YEp195-GAL-His-HA-DDC2 or YEp195-GAL-His-HA-DDC2-S4. Transformed cells were grown in sucrose media (2% sucrose 0.05% glucose) to a log-phase and incubated with 2% galactose for 5 hr to induce expression from the *GAL* promoter. Crude extracts were prepared from 10 gram of cells in 50 ml of buffer A (20 mM Tris-HCl [pH 8], 10% glycerol, 3 mM DTT, 0.1% Triton X-100) containing 1 mM EDTA, 100 mM NaCl and inhibitors (1 mM phenylmethylsulfonyl fluoride (PMSF), 1 μg/ml leupeptin, 1 mM benzamide, 1 mM  $\text{Na}_3\text{VO}_4$ ) by vortexing with 600 μl of glass beads. After clearing by centrifugation, supernatant was incubated with 2 ml of ANTI-FLAG-M2 affinity agarose (Sigma) for 2 hr. Resin was washed with 20 ml of buffer A containing 400 mM NaCl, 10 ml of buffer A containing 100 mM NaCl, 20 ml of buffer A containing 100 mM NaCl, 5 mM  $\text{MgCl}_2$  and 1mM ATP, and 20 ml of buffer A containing 100 mM NaCl. FLAG-tagged protein was eluted with 4 ml of buffer A containing 100 mM NaCl, 300 μg/ml of FLAG-peptide (Sigma), 2.5 mM  $\text{MgCl}_2$ , 5U of Benzonase (Millipore). The FLAG-eluate was incubated with 1 ml of Ni-NTA-agarose (Clontech) for one hour, washed with 5 ml of buffer A containing 100 mM NaCl. Bound protein was eluted with 1.5 ml of buffer A containing 150 mM NaCl and 300 mM imidazole and then concentrated using a Vivaspin 500 column (GE Healthcare) with buffer A containing 150 mM NaCl. All the protein purification procedures were performed at 4°C.

## Purification of MBP-Ddc2 and MBP-Ddc2-S4 protein

The coding sequences for *DDC2* and *ddc2-S4* were amplified by PCR using YCpT-myc-DDC2 [82] and YCp-myc-DDC2-S4 [49] with the primer pair KS3620 and KSX001, and cloned into the BamHI and Sall sites of pMAL-c2X (New England Biolabs) to generate the plasmid pMAL-Ddc2 and pMAL-Ddc2-S4, respectively. Proteins were expressed in *E. coli* Rosetta (Novagen) after the incubation with 1 mM IPTG at 30°C for 4 hr. The cell pellet from one liter of culture was suspended in 50 ml of buffer M (25 mM Tris-HCl pH 7.5], 10% glycerol, 0.5 mM EDTA, 1 mM DTT) containing 300 mM NaCl and protease inhibitors (leupeptin and pepstatin A at 5 μg/ml each, 1 mM PMSF). After sonication, crude cell lysates were clarified by centrifugation and then incubated with pre-equilibrated 1 ml of amylose resin (New England Biolabs) for 2 hr. After washing with buffer M containing 1 M NaCl, bound proteins were eluted with 2 ml of buffer M containing 300 mM NaCl and 10 mM maltose. Eluates were pooled and concentrated using Vivaspin 500 columns.

## Binding of Mec1-Ddc2 or MBP-Ddc2 to ssDNA

Streptavidin beads (4 μl; Pierce) coated with biotinylated oligonucleotides were incubated with RPA for 30 min and further incubated for 30 min after the addition of Mec1-Ddc2 or

MBP-Ddc2 proteins in 500  $\mu$ l of the binding buffer B (20 mM Tris-HCl [pH 7.5], 100 mM NaCl, 0.01% NP-40, 10% glycerol, 100  $\mu$ g/ml bovine serum albumin) at 30°C. Beads were recovered and subjected to immunoblotting analysis.

### Interaction of Mec1-Ddc2 with RPA

Mec1-Ddc2 and RPA were incubated with or without oligonucleotides in the binding buffer B containing ANTI-FLAG-M2 affinity agarose for 30 min at 30°C. Beads were subjected to immunoblotting analysis.

### Mec1 kinase assay

Kinase reactions were carried out by the addition of Mec1-Ddc2 or Mec1-Ddc2-S4 in 40  $\mu$ l (final volume) of the kinase buffer (20 mM HEPES-KOH [pH 7.5], 10 mM NaCl, 10 mM MgCl<sub>2</sub>, 4 mM MnCl<sub>2</sub>, 50  $\mu$ M ATP) containing 5  $\mu$ Ci [ $\gamma$ -<sup>32</sup>P] ATP (3,000 Ci/mmol) and 400 nM GST-Rad53. To detect RPA phosphorylation, GST-Rad53 was omitted in kinase reactions. GST-Rad53 was purified as described [49]. Each reaction contains 5 nM purified Mec1-Ddc2 or Mec1-Ddc2-S4. Before initiating kinase reactions, Mec1-Ddc2 or Mec1-Ddc2-S4 was incubated with RPA, ssDNA/oligonucleotide or RPA-ssDNA complex in 4  $\mu$ l of 15 mM Tris-HCl [pH 7.5], 100 mM NaCl, 0.025 mM EDTA for 15 min at 30°C. RPA-ssDNA complex was prepared by mixing RPA and ssDNA/oligonucleotide for 30 min at 30°C. After 10 min of incubation at 30°C, the kinase reactions were terminated by the addition of 5x SDS-sample buffer. The reaction mixtures were separated on SDS-polyacrylamide gels, and phosphorylation was quantified with a phosphor imager system (Typhoon 8600, GE Healthcare).

### Other methods

Cells were incubated with  $\alpha$ -factor (6  $\mu$ g/ml) or nocodazole (15  $\mu$ g/ml) for 2 hr to synchronize at G1 or G2/M, respectively. Chromatin immunoprecipitation assay and immunoblotting analysis were carried out as described [49, 78]. DNA flow cytometry was carried out by using FACSCalibur (BD Biosciences) [49]. Budding yeast RPA protein was purified as described [83]. Anti-Rfa1 and anti-Rfa2 antibodies were obtained from Steve Brill (Rutgers, Piscataway). Anti-Rad53 antibody (EL7.E1) was purchased from Abcam. The ribbon diagram of Ddc2 was generated by PyMOL (Palo Alto, CA) using the PDB data base (PDB ID: 5X60).

### Supporting information

**S1 Fig. Overview of the resection assay.** DNA end resection generates ssDNA. EcoRI restriction sites become resistant to restriction digestion once converted to ssDNA. PCR amplifies only EcoRI resistant ssDNA.

(TIF)

**S2 Fig. Purification of Mec1-Ddc2 and Mec1-Ddc2-S4.** Purified Mec1-Ddc2 and Mec1-Ddc2-S4 were separated on SDS-PAGE and stained by Coomassie Brilliant Blue. Mec1-Ddc2 (lane 1) and Mec1-Ddc2-S4 (lane 2) were purified through a two-step ANTI-FLAG-M2 and Ni-NTA column purification.

(TIF)

**S3 Fig. The amount of RPA in purified Mec1-Ddc2 complex.** Kinase reactions (40  $\mu$ l) were carried out with Mec1-Ddc2 (5 nM or 0.2 pmol) using various concentrations (amounts) of RPA in the absence or presence of bio-oligo(dN)<sub>80</sub> (12.5 nM) as in Fig 7B. Kinase activities of Mec1-Ddc2, normalized to that observed with Mec1-Ddc2 alone, are shown in comparison

with those in the presence of RPA or ssDNA. The amount of RPA in purified Mec1-Ddc2 protein was analyzed by immunoblotting analysis with anti-Rfa2 antibody. Purified RPA was loaded as reference.

(TIF)

**S4 Fig. RPA phosphorylation by Mec1-Ddc2 in the presence or absence of ssDNA.** Kinase reactions were carried out using Mec1-Ddc2 (5 nM) with various concentrations of RPA in the absence or presence of bio-oligo(dN)<sub>80</sub> (125 nM).

(TIF)

**S5 Fig. Enlarged view of Mec1-Ddc2 homodimerization interface.** Ddc2 is shown in green and the Mec1 N-terminal  $\alpha$ -solenoid of another Mec1-Ddc2 heterodimer is highlighted in cyan. The interaction of Lys<sup>263</sup> of Ddc2 with Asp<sup>322</sup> and Gln<sup>323</sup> of Mec1 is shown.

(TIF)

**S6 Fig. Effect of biotinylated oligonucleotide on Mec1 activation.** Kinase reactions were carried out with Mec1-Ddc2 (5 nM) using various concentrations of biotinylated or unmodified oligo(dN)<sub>80</sub>. Incorporation of <sup>32</sup>P into GST-Rad53 was analyzed as in Fig 6A.

(TIF)

**S7 Fig. Competition between RPA and ssDNA-bound RPA for Mec1-Ddc2 binding.**

Because Mec1-Ddc2 interacts with RPA independently of ssDNA, ssDNA-free RPA could compete with ssDNA-bound RPA for Mec1-Ddc2 binding.

(TIF)

**S1 Table. Strains used in this study.**

(DOCX)

**S2 Table. Oligonucleotides in this study.**

(DOCX)

## Acknowledgments

We thank Avik Ghosh for set-up of Mec1 purification, Steven Brill and Peter Burgers for sending materials, John Kang for critical reading, Hiro Araki, Steven Brill, Atul Khataokar, Eiji Ohashi and Toshiki Tsurimoto for discussion and suggestion, Satoshi Matsuura for encouragement.

## Author Contributions

**Conceptualization:** Himadri Biswas, Katsunori Sugimoto.

**Data curation:** Himadri Biswas, Greicy Goto.

**Formal analysis:** Himadri Biswas, Greicy Goto, Katsunori Sugimoto.

**Funding acquisition:** Patrick Sung, Katsunori Sugimoto.

**Investigation:** Katsunori Sugimoto.

**Methodology:** Weibin Wang, Patrick Sung.

**Resources:** Weibin Wang, Patrick Sung.

**Writing – original draft:** Himadri Biswas, Weibin Wang, Patrick Sung, Katsunori Sugimoto.

## References

1. Ciccia A, Elledge SJ. The DNA damage response: making it safe to play with knives. *Mol Cell*. 2010; 40(2):179–204. <https://doi.org/10.1016/j.molcel.2010.09.019> PMID: 20965415
2. Harper JW, Elledge SJ. The DNA damage response: ten years after. *Mol Cell*. 2007; 28(5):739–45. <https://doi.org/10.1016/j.molcel.2007.11.015> PMID: 18082599.
3. Blackford AN, Jackson SP. ATM, ATR, and DNA-PK: The Trinity at the Heart of the DNA Damage Response. *Mol Cell*. 2017; 66(6):801–17. <https://doi.org/10.1016/j.molcel.2017.05.015> PMID: 28622525.
4. Yazinski SA, Zou L. Functions, Regulation, and Therapeutic Implications of the ATR Checkpoint Pathway. *Annu Rev Genet*. 2016; 50:155–73. <https://doi.org/10.1146/annurev-genet-121415-121658> PMID: 27617969.
5. Saldivar JC, Cortez D, Cimprich KA. The essential kinase ATR: ensuring faithful duplication of a challenging genome. *Nat Rev Mol Cell Biol*. 2017; 18(10):622–36. <https://doi.org/10.1038/nrm.2017.67> PMID: 28811666
6. Paull TT. Mechanisms of ATM Activation. *Annu Rev Biochem*. 2015. <https://doi.org/10.1146/annurev-biochem-060614-034335> PMID: 25580527.
7. Smith GC, Jackson SP. The DNA-dependent protein kinase. *Genes Dev*. 1999; 13(8):916–34. <https://doi.org/10.1101/gad.13.8.916> PMID: 10215620.
8. Wold MS. Replication protein A: a heterotrimeric, single-stranded DNA-binding protein required for eukaryotic DNA metabolism. *Annu Rev Biochem*. 1997; 66:61–92. <https://doi.org/10.1146/annurev-biochem.66.1.61> PMID: 9242902
9. Makiniemi M, Hillukkala T, Tuusa J, Reini K, Vaara M, Huang D, et al. BRCT domain-containing protein TopBP1 functions in DNA replication and damage response. *J Biol Chem*. 2001; 276(32):30399–406. Epub 2001/06/08. <https://doi.org/10.1074/jbc.M102245200> PMID: 11395493.
10. Garcia V, Furuya K, Carr AM. Identification and functional analysis of TopBP1 and its homologs. *DNA Repair (Amst)*. 2005; 4(11):1227–39. Epub 2005/05/18. <https://doi.org/10.1016/j.dnarep.2005.04.001> PMID: 15897014.
11. Wardlaw CP, Carr AM, Oliver AW. TopBP1: A BRCT-scaffold protein functioning in multiple cellular pathways. *DNA Repair (Amst)*. 2014; 22:165–74. Epub 2014/08/05. <https://doi.org/10.1016/j.dnarep.2014.06.004> PMID: 25087188.
12. Acevedo J, Yan S, Michael WM. Direct Binding to Replication Protein A (RPA)-coated Single-stranded DNA Allows Recruitment of the ATR Activator TopBP1 to Sites of DNA Damage. *J Biol Chem*. 2016; 291(25):13124–31. <https://doi.org/10.1074/jbc.M116.729194> PMID: 27129245
13. Kumagai A, Lee J, Yoo HY, Dunphy WG. TopBP1 activates the ATR-ATRIP complex. *Cell*. 2006; 124(5):943–55. <https://doi.org/10.1016/j.cell.2005.12.041> PMID: 16530042.
14. Bass TE, Luzwick JW, Kavanaugh G, Carroll C, Dungrawala H, Glick GG, et al. ETAA1 acts at stalled replication forks to maintain genome integrity. *Nat Cell Biol*. 2016; 18(11):1185–95. <https://doi.org/10.1038/ncb3415> PMID: 27723720
15. Haahr P, Hoffmann S, Tollenare MA, Ho T, Toledo LI, Mann M, et al. Activation of the ATR kinase by the RPA-binding protein ETAA1. *Nat Cell Biol*. 2016; 18(11):1196–207. <https://doi.org/10.1038/ncb3422> PMID: 27723717.
16. Lee YC, Zhou Q, Chen J, Yuan J. RPA-Binding Protein ETAA1 Is an ATR Activator Involved in DNA Replication Stress Response. *Curr Biol*. 2016; 26(24):3257–68. <https://doi.org/10.1016/j.cub.2016.10.030> PMID: 27818175
17. Zou L, Elledge SJ. Sensing DNA damage through ATRIP recognition of RPA-ssDNA complexes. *Science*. 2003; 300:1542–8. <https://doi.org/10.1126/science.1083430> PMID: 12791985
18. Nakada D, Hirano Y, Tanaka Y, Sugimoto K. Role of the C terminus of mec1 checkpoint kinase in its localization to sites of DNA damage. *Mol Biol Cell*. 2005; 16(11):5227–35. <https://doi.org/10.1091/mbc.E05-05-0405> PMID: 16148046.
19. Ogiwara H, Ui A, Onoda F, Tada S, Enomoto T, Seki M. Dpb11, the budding yeast homolog of TopBP1, functions with the checkpoint clamp in recombination repair. *Nucleic Acids Res*. 2006; 34(11):3389–98. <https://doi.org/10.1093/nar/gkl411> PMID: 16840526
20. Germann SM, Oestergaard VH, Haas C, Salis P, Motegi A, Lisby M. Dpb11/TopBP1 plays distinct roles in DNA replication, checkpoint response and homologous recombination. *DNA Repair (Amst)*. 2011; 10(2):210–24. <https://doi.org/10.1016/j.dnarep.2010.11.001> PMID: 21130053.
21. Majka J, Niedziela-Majka A, Burgers PM. The checkpoint clamp activates Mec1 kinase during initiation of the DNA damage checkpoint. *Mol Cell*. 2006; 24(6):891–901. <https://doi.org/10.1016/j.molcel.2006.11.027> PMID: 17189191

22. Navadgi-Patil VM, Burgers PM. Yeast DNA replication protein Dpb11 activates the Mec1/ATR checkpoint kinase. *J Biol Chem.* 2008; 283(51):35853–9. Epub 2008/10/17. <https://doi.org/10.1074/jbc.M807435200> PMID: 18922789.
23. Navadgi-Patil VM, Burgers PM. The unstructured C-terminal tail of the 9-1-1 clamp subunit Ddc1 activates Mec1/ATR via two distinct mechanisms. *Mol Cell.* 2009; 36(5):743–53. <https://doi.org/10.1016/j.molcel.2009.10.014> PMID: 20005839
24. Navadgi-Patil VM, Kumar S, Burgers PM. The unstructured C-terminal tail of yeast Dpb11 (human TopBP1) protein is dispensable for DNA replication and the S phase checkpoint but required for the G2/M checkpoint. *J Biol Chem.* 2011; 286(47):40999–1007. <https://doi.org/10.1074/jbc.M111.283994> PMID: 21956112
25. Mordes DA, Nam EA, Cortez D. Dpb11 activates the Mec1-Ddc2 complex. *Proc Natl Acad Sci U S A.* 2008; 105(48):18730–4. <https://doi.org/10.1073/pnas.0806621105> PMID: 19028869
26. Kumar S, Burgers PM. Lagging strand maturation factor Dna2 is a component of the replication checkpoint initiation machinery. *Genes Dev.* 2013; 27(3):313–21. <https://doi.org/10.1101/gad.204750.112> PMID: 23355394
27. Lanz MC, Oberly S, Sanford EJ, Sharma S, Chabes A, Smolka MB. Separable roles for Mec1/ATR in genome maintenance, DNA replication, and checkpoint signaling. *Genes Dev.* 2018; 32(11–12):822–35. <https://doi.org/10.1101/gad.308148.117> PMID: 29899143.
28. Elledge SJ. Cell cycle checkpoints: preventing an identity crisis. *Science.* 1996; 274:1664–72. <https://doi.org/10.1126/science.274.5293.1664> PMID: 8939848
29. Zhou B-BS, Elledge SJ. The DNA damage response: putting checkpoints in perspective. *Nature.* 2000; 408:433–9. <https://doi.org/10.1038/35044005> PMID: 11100718
30. Schwartz MF, Duong JK, Sun Z, Morrow JS, Pradhan D, Stern DF. Rad9 phosphorylation sites couple Rad53 to the *Saccharomyces cerevisiae* DNA damage checkpoint. *Mol Cell.* 2002; 9:1055–65. PMID: 12049741
31. Sweeney FD, Yang F, Chi A, Shabanowitz J, Hunt DF, Durocher D. *Saccharomyces cerevisiae* Rad9 acts as a Mec1 adaptor to allow Rad53 activation. *Curr Biol.* 2005; 15(15):1364–75. <https://doi.org/10.1016/j.cub.2005.06.063> PMID: 16085488.
32. Osborn AJ, Elledge SJ. Mrc1 is a replication fork component whose phosphorylation in response to DNA replication stress activates Rad53. *Genes Dev.* 2003; 17:1755–67. <https://doi.org/10.1101/gad.1098303> PMID: 12865299
33. Chen SH, Zhou H. Reconstitution of Rad53 activation by Mec1 through adaptor protein Mrc1. *J Biol Chem.* 2009; 284(28):18593–604. Epub 2009/05/22. <https://doi.org/10.1074/jbc.M109.018242> PMID: 19457865
34. Vialard JE, Gilbert CS, Green CM, Lowndes NF. The budding yeast Rad9 checkpoint protein is subjected to Mec1/Tel1-dependent hyperphosphorylation and interacts with Rad53 after DNA damage. *EMBO J.* 1998; 17:5679–88. <https://doi.org/10.1093/emboj/17.19.5679> PMID: 9755168
35. Alcasabas AA, Osborn AJ, Bachant J, Hu F, Werler PJ, Bousset K, et al. Mrc1 transduces signals of DNA replication stress to activate Rad53. *Nat Cell Biol.* 2001; 3(11):958–65. Epub 2001/11/21. <https://doi.org/10.1038/ncb1101-958> PMID: 11715016.
36. Katou Y, Kanoh Y, Bando M, Noguchi H, Tanaka H, Ashikari T, et al. S-phase checkpoint proteins Tof1 and Mrc1 form a stable replication-pausing complex. *Nature.* 2003; 424:1073–83.
37. Bando M, Katou Y, Komata M, Tanaka H, Itoh T, Sutani T, et al. Csm3, Tof1, and Mrc1 form a heterotrimeric mediator complex that associates with DNA replication forks. *J Biol Chem.* 2009; 284(49):34355–65. Epub 2009/10/13. <https://doi.org/10.1074/jbc.M109.065730> PMID: 19819872
38. Lou H, Komata M, Katou Y, Guan Z, Reis CC, Budd M, et al. Mrc1 and DNA polymerase epsilon function together in linking DNA replication and the S phase checkpoint. *Mol Cell.* 2008; 32(1):106–17. Epub 2008/10/15. <https://doi.org/10.1016/j.molcel.2008.08.020> PMID: 18851837
39. Pfander B, Diffley JF. Dpb11 coordinates Mec1 kinase activation with cell cycle-regulated Rad9 recruitment. *EMBO J.* 2011; 30(24):4897–907. <https://doi.org/10.1038/emboj.2011.345> PMID: 21946560
40. Cussiol JR, Jablonowski CM, Yimit A, Brown GW, Smolka MB. Dampening DNA damage checkpoint signalling via coordinated BRCT domain interactions. *EMBO J.* 2015; 34(12):1704–17. Epub 2015/04/22. <https://doi.org/10.15252/emboj.201490834> PMID: 25896509
41. Wysocki R, Javaheri A, Allard S, Sha F, Cote J, Kron SJ. Role of Dot1-dependent histone H3 methylation in G1 and S phase DNA damage checkpoint functions of Rad9. *Mol Cell Biol.* 2005; 25(19):8430–43. Epub 2005/09/17. <https://doi.org/10.1128/MCB.25.19.8430-8443.2005> PMID: 16166626
42. Grenon M, Costelloe T, Jimeno S, O'Shaughnessy A, Fitzgerald J, Zgheib O, et al. Docking onto chromatin via the *Saccharomyces cerevisiae* Rad9 Tudor domain. *Yeast.* 2007; 24(2):105–19. Epub 2007/01/24. <https://doi.org/10.1002/yea.1441> PMID: 17243194.

43. Hammet A, Magjill C, Heierhorst J, Jackson SP. Rad9 BRCT domain interaction with phosphorylated H2AX regulates the G1 checkpoint in budding yeast. *EMBO Rep.* 2007; 8(9):851–7. Epub 2007/08/28. <https://doi.org/10.1038/sj.embor.7401036> PMID: 17721446.
44. Granata M, Lazzaro F, Novarina D, Panigada D, Puddu F, Abreu CM, et al. Dynamics of Rad9 chromatin binding and checkpoint function are mediated by its dimerization and are cell cycle-regulated by CDK1 activity. *PLoS Genet.* 2010; 6(8). <https://doi.org/10.1371/journal.pgen.1001047> PMID: 20700441
45. Nguyen AT, Zhang Y. The diverse functions of Dot1 and H3K79 methylation. *Genes Dev.* 2011; 25(13):1345–58. Epub 2011/07/05. <https://doi.org/10.1101/gad.2057811> PMID: 21724828
46. Shroff R, Arbel-Eden A, Pilch D, Ira G, Bonner WM, Petrini JH, et al. Distribution and dynamics of chromatin modification induced by a defined DNA double-strand break. *Curr Biol.* 2004; 14(19):1703–11. Epub 2004/10/02. <https://doi.org/10.1016/j.cub.2004.09.047> PMID: 15458641.
47. Lee CS, Lee K, Legube G, Haber JE. Dynamics of yeast histone H2A and H2B phosphorylation in response to a double-strand break. *Nat Struct Mol Biol.* 2014; 21(1):103–9. Epub 2013/12/18. <https://doi.org/10.1038/nsmb.2737> PMID: 24336221
48. Puddu F, Granata M, Di Nola L, Balestrini A, Piergiovanni G, Lazzaro F, et al. Phosphorylation of the budding yeast 9-1-1 complex is required for Dpb11 function in the full activation of the UV-induced DNA damage checkpoint. *Mol Cell Biol.* 2008; 28(15):4782–93. Epub 2008/06/11. <https://doi.org/10.1128/MCB.00330-08> PMID: 18541674
49. Bandhu A, Kang J, Fukunaga K, Goto G, Sugimoto K. Ddc2 Mediates Mec1 Activation through a Ddc1- or Dpb11-Independent Mechanism. *PLoS Genet.* 2014; 10(2):e1004136. <https://doi.org/10.1371/journal.pgen.1004136> PMID: 24586187
50. Ferrari M, Dibitetto D, De Gregorio G, Eapen VV, Rawal CC, Lazzaro F, et al. Functional interplay between the 53BP1-ortholog Rad9 and the Mre11 complex regulates resection, end-tethering and repair of a double-strand break. *PLoS Genet.* 2015; 11(1):e1004928. Epub 2015/01/09. <https://doi.org/10.1371/journal.pgen.1004928> PMID: 25569305
51. Zierhut C, Diffley JF. Break dosage, cell cycle stage and DNA replication influence DNA double strand break response. *EMBO J.* 2008; 27(13):1875–85. Epub 2008/05/31. <https://doi.org/10.1038/emboj.2008.111> PMID: 18511906
52. Clerici M, Trovesi C, Galbiati A, Lucchini G, Longhese MP. Mec1/ATR regulates the generation of single-stranded DNA that attenuates Tel1/ATM signaling at DNA ends. *EMBO J.* 2014; 33(3):198–216. Epub 2013/12/21. <https://doi.org/10.1002/emboj.201386041> PMID: 24357557
53. Melo JA, Cohen J, Toczyski DP. Two checkpoint complexes are independently recruited to sites of DNA damage *in vivo*. *Genes & Dev.* 2001; 21:2809–21.
54. Kondo T, Wakayama T, Naiki T, Matsumoto K, Sugimoto K. Recruitment of Mec1 and Ddc1 checkpoint proteins to double-strand breaks through distinct mechanisms. *Science.* 2001; 5543:867–70.
55. Berens TJ, Toczyski DP. Colocalization of Mec1 and Mrc1 is sufficient for Rad53 phosphorylation *in vivo*. *Mol Biol Cell.* 2012; 23(6):1058–67. <https://doi.org/10.1091/mbc.E11-10-0852> PMID: 22298423
56. Bastos de Oliveira FM, Kim D, Cussiol JR, Das J, Jeong MC, Doerfler L, et al. Phosphoproteomics reveals distinct modes of Mec1/ATR signaling during DNA replication. *Mol Cell.* 2015; 57(6):1124–32. <https://doi.org/10.1016/j.molcel.2015.01.043> PMID: 25752575
57. Brush GS, Kelly TJ. Phosphorylation of the replication protein A large subunit in the *Saccharomyces cerevisiae* checkpoint response. *Nucleic Acids Res.* 2000; 28(19):3725–32. <https://doi.org/10.1093/nar/28.19.3725> PMID: 11000264.
58. Bartrand AJ, Iyasu D, Brush GS. DNA stimulates Mec1-mediated phosphorylation of replication protein A. *J Biol Chem.* 2004; 279(25):26762–7. <https://doi.org/10.1074/jbc.M312353200> PMID: 15078888.
59. Binz SK, Sheehan AM, Wold MS. Replication protein A phosphorylation and the cellular response to DNA damage. *DNA Repair (Amst).* 2004; 3(8–9):1015–24. Epub 2004/07/29. <https://doi.org/10.1016/j.dnarep.2004.03.028> PMID: 15279788.
60. Unsal-Kacmaz K, Sancar A. Quaternary structure of ATR and effects of ATRIP and replication protein A on its DNA binding and kinase activities. *Mol Cell Biol.* 2004; 24(3):1292–300. Epub 2004/01/20. <https://doi.org/10.1128/MCB.24.3.1292-1300.2003> PMID: 14729973
61. Wang X, Ran T, Zhang X, Xin J, Zhang Z, Wu T, et al. 3.9 A structure of the yeast Mec1-Ddc2 complex, a homolog of human ATR-ATRIP. *Science.* 2017; 358(6367):1206–9. <https://doi.org/10.1126/science.aan8414> PMID: 29191911.
62. Rouse J, Jackson SP. Lcd1p recruits Mec1p to DNA lesions *in vitro* and *in vivo*. *Mol Cell.* 2002; 9:857–69. PMID: 11983176
63. Ball HL, Ehrhardt MR, Mordes DA, Glick GG, Chazin WJ, Cortez D. Function of a conserved checkpoint recruitment domain in ATRIP proteins. *Mol Cell Biol.* 2007; 27(9):3367–77. <https://doi.org/10.1128/MCB.02238-06> PMID: 17339343

64. Deshpande I, Seeber A, Shimada K, Keusch JJ, Gut H, Gasser SM. Structural Basis of Mec1-Ddc2-RPA Assembly and Activation on Single-Stranded DNA at Sites of Damage. *Mol Cell*. 2017; 68(2):431–45 e5. <https://doi.org/10.1016/j.molcel.2017.09.019> PMID: 29033322.
65. Lindsey-Boltz LA, Reardon JT, Wold MS, Sancar A. In vitro analysis of the role of replication protein A (RPA) and RPA phosphorylation in ATR-mediated checkpoint signaling. *J Biol Chem*. 2012; 287(43):36123–31. Epub 2012/09/06. <https://doi.org/10.1074/jbc.M112.407825> PMID: 22948311
66. Ohouo PY, Bastos de Oliveira FM, Almeida BS, Smolka MB. DNA damage signaling recruits the Rtt107-Slx4 scaffolds via Dpb11 to mediate replication stress response. *Mol Cell*. 2010; 39(2):300–6. Epub 2010/07/31. <https://doi.org/10.1016/j.molcel.2010.06.019> PMID: 20670896.
67. Mordes DA, Glick GG, Zhao R, Cortez D. TopBP1 activates ATR through ATRIP and a PIKK regulatory domain. *Genes Dev*. 2008; 22(11):1478–89. Epub 2008/06/04. <https://doi.org/10.1101/gad.1666208> PMID: 18519640.
68. Paciotti V, Lucchini G, Plevani P, Longhese MP. Mec1p is essential for phosphorylation of the yeast DNA damage checkpoint protein Ddc1p, which physically interacts with Mec3p. *EMBO J*. 1998; 17:4199–209. <https://doi.org/10.1093/emboj/17.14.4199> PMID: 9670034
69. Chen X, Niu H, Chung WH, Zhu Z, Papusha A, Shim EY, et al. Cell cycle regulation of DNA double-strand break end resection by Cdk1-dependent Dna2 phosphorylation. *Nat Struct Mol Biol*. 2011; 18(9):1015–9. Epub 2011/08/16. <https://doi.org/10.1038/nsmb.2105> PMID: 21841787
70. Choi JH, Lindsey-Boltz LA, Kemp M, Mason AC, Wold MS, Sancar A. Reconstitution of RPA-covered single-stranded DNA-activated ATR-Chk1 signaling. *Proc Natl Acad Sci U S A*. 2010; 107(31):13660–5. <https://doi.org/10.1073/pnas.1007856107> PMID: 20616048
71. Niu H, Chung WH, Zhu Z, Kwon Y, Zhao W, Chi P, et al. Mechanism of the ATP-dependent DNA end-resection machinery from *Saccharomyces cerevisiae*. *Nature*. 2010; 467(7311):108–11. Epub 2010/09/03. <https://doi.org/10.1038/nature09318> PMID: 20811460
72. Cejka P, Cannavo E, Polaczek P, Masuda-Sasa T, Pokharel S, Campbell JL, et al. DNA end resection by Dna2-Sgs1-RPA and its stimulation by Top3-Rmi1 and Mre11-Rad50-Xrs2. *Nature*. 2010; 467(7311):112–6. <https://doi.org/10.1038/nature09355> PMID: 20811461
73. Cannavo E, Cejka P, Kowalczykowski SC. Relationship of DNA degradation by *Saccharomyces cerevisiae* exonuclease 1 and its stimulation by RPA and Mre11-Rad50-Xrs2 to DNA end resection. *Proc Natl Acad Sci U S A*. 2013; 110(18):E1661–8. <https://doi.org/10.1073/pnas.1305166110> PMID: 23589858
74. Chen H, Lisby M, Symington LS. RPA coordinates DNA end resection and prevents formation of DNA hairpins. *Mol Cell*. 2013; 50(4):589–600. <https://doi.org/10.1016/j.molcel.2013.04.032> PMID: 23706822
75. Taylor MRG, Yeeles JTP. The Initial Response of a Eukaryotic Replisome to DNA Damage. *Mol Cell*. 2018; 70(6):1067–80 e12. <https://doi.org/10.1016/j.molcel.2018.04.022> PMID: 29944888
76. Yates LA, Aramayo RJ, Pokhrel N, Caldwell CC, Kaplan JA, Perera RL, et al. A structural and dynamic model for the assembly of Replication Protein A on single-stranded DNA. *Nature communications*. 2018; 9(1):5447. Epub 2018/12/24. <https://doi.org/10.1038/s41467-018-07883-7> PMID: 30575763
77. Pokhrel N, Caldwell CC, Corless EI, Tillison EA, Tibbs J, Jovic N, et al. Dynamics and selective remodeling of the DNA-binding domains of RPA. *Nat Struct Mol Biol*. 2019; 26(2):129–36. Epub 2019/02/07. <https://doi.org/10.1038/s41594-018-0181-y> PMID: 30723327
78. Goto GH, Ogi H, Biswas H, Ghosh A, Tanaka S, Sugimoto K. Two separate pathways regulate protein stability of ATM/ATR-related protein kinases Mec1 and Tel1 in budding yeast. *PLoS Genet*. 2017; 13(8):e1006873. <https://doi.org/10.1371/journal.pgen.1006873> PMID: 28827813
79. Reid RJ, Lisby M, Rothstein R. Cloning-free genome alterations in *Saccharomyces cerevisiae* using adaptamer-mediated PCR. *Methods Enzymol*. 2002; 350:258–77. [https://doi.org/10.1016/S0076-6879\(02\)50968-x](https://doi.org/10.1016/S0076-6879(02)50968-x) PMID: 12073317
80. Janke C, Magiera MM, Rathfelder N, Taxis C, Reber S, Maekawa H, et al. A versatile toolbox for PCR-based tagging of yeast genes: new fluorescent proteins, more markers and promoter substitution cassettes. *Yeast*. 2004; 21(11):947–62. Epub 2004/08/31. <https://doi.org/10.1002/yea.1142> PMID: 15334558.
81. Fukunaga K, Hirano Y, Sugimoto K. Subtelomere-binding protein Tbf1 and telomere-binding protein Rap1 collaborate to inhibit localization of the Mre11 complex to DNA ends in budding yeast. *Mol Biol Cell*. 2012; 23(2):347–59. <https://doi.org/10.1091/mbc.E11-06-0568> PMID: 22130795
82. Wakayama T, Kondo T, Ando S, Matsumoto K, Sugimoto K. Pie1, a protein interacting with Mec1, controls cell growth and checkpoint responses in *Saccharomyces cerevisiae*. *Mol Cell Biol*. 2001; 21:755–64. <https://doi.org/10.1128/MCB.21.3.755-764.2001> PMID: 11154263
83. Van Komen S, Macris M, Sehorn MG, Sung P. Purification and assays of *Saccharomyces cerevisiae* homologous recombination proteins. *Methods Enzymol*. 2006; 408:445–63. [https://doi.org/10.1016/S0076-6879\(06\)08028-1](https://doi.org/10.1016/S0076-6879(06)08028-1) PMID: 16793386.